

Combined Report from GMn Ph.D. Students



Provakar Datta

(On behalf of the GMn Analysis Team)

SBS-GMn/nTPE Analysis Team



Ralph Marinaro, GU
(BigBite Hodoscope)



Nathaniel Lashley, HU
(Beamline)



John Boyd*, UVA
(GEM)



Sebastian Seeds*, UConn
(Hadron Calorimeter)



Anuruddha Rathnayake, UVA
(GEM)



Maria Satnik, W&M
(GRINCH)



Ezekiel Wertz*, W&M
(GEM)



Provakar Datta, UConn
(BigBite Calorimeter)

- Eric Fuchey, W&M (Analysis Coordinator)
- Andrew Puckett, UConn
- David Armstrong, W&M
- Bogdan Wojtsekhowski, JLab
- Nilanga Liyanage, UVA
- Arun Tadepalli, JLab
- ...
- Mark Jones, JLab

Outline

- Brief Overview
- Physics Analysis Methodology
- Extraction of Experimental Observable
- Systematic Uncertainty Quantification
- Preliminary Results
- Summary and outlook

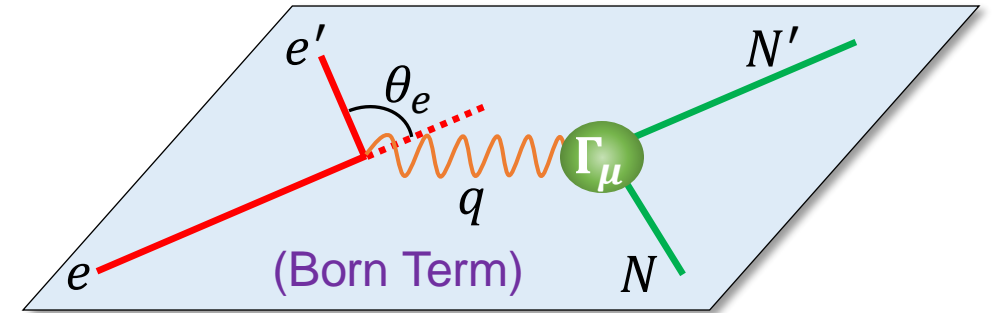
Elastic eN Scattering and the Nucleon EMFFs

- SBS-GMn (E12-09-019) ran in Jefferson Lab's Experimental Hall A from Fall 2021 to February 2022.

❖ **Goal:** High precision measurement of G_M^n at $Q^2 = 3, 4.5, 7.4, 9.9, \& 13.6$ (GeV/c)².

- Nucleon vertex (elastic $e-N$ scattering):

$$\Gamma_\mu(q) = \gamma_\mu \underbrace{F_1(-q^2)}_{\text{Dirac FF}} + \frac{i\sigma_{\mu\nu}q^\nu}{2M_N} \underbrace{F_2(-q^2)}_{\text{Pauli FF}}$$



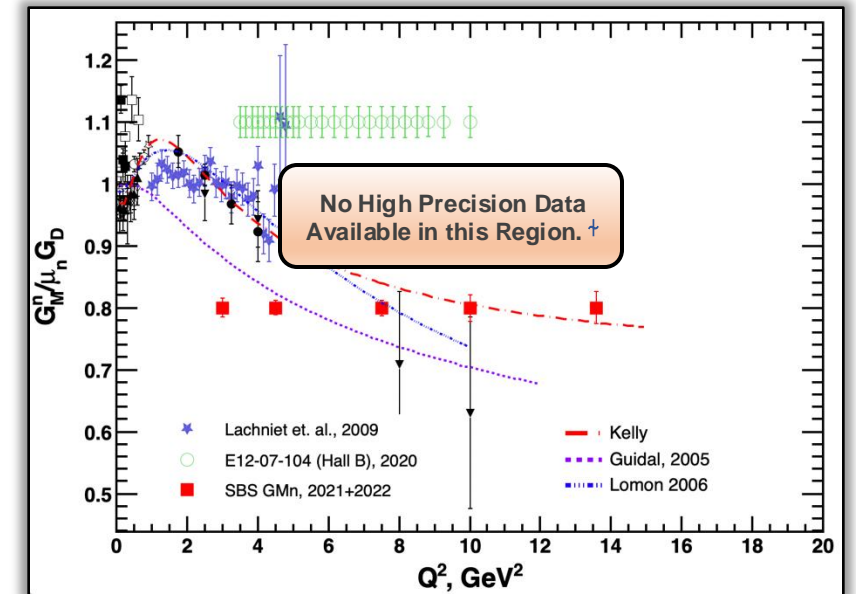
- Defining Sachs Form Factors (FFs): $\begin{cases} G_E(Q^2) \equiv F_1(Q^2) - \tau F_2(Q^2) \\ G_M(Q^2) \equiv F_1(Q^2) + F_2(Q^2) \end{cases}$

- G_E, G_M : Sachs Electric and Magnetic FFs, respectively.

- Differential Cross Section:

$$\frac{d\sigma}{d\Omega} = \frac{\sigma_{Mott}}{1 + \tau} \left(G_E^2(Q^2) + \frac{\tau}{\epsilon} G_M^2(Q^2) \right)$$

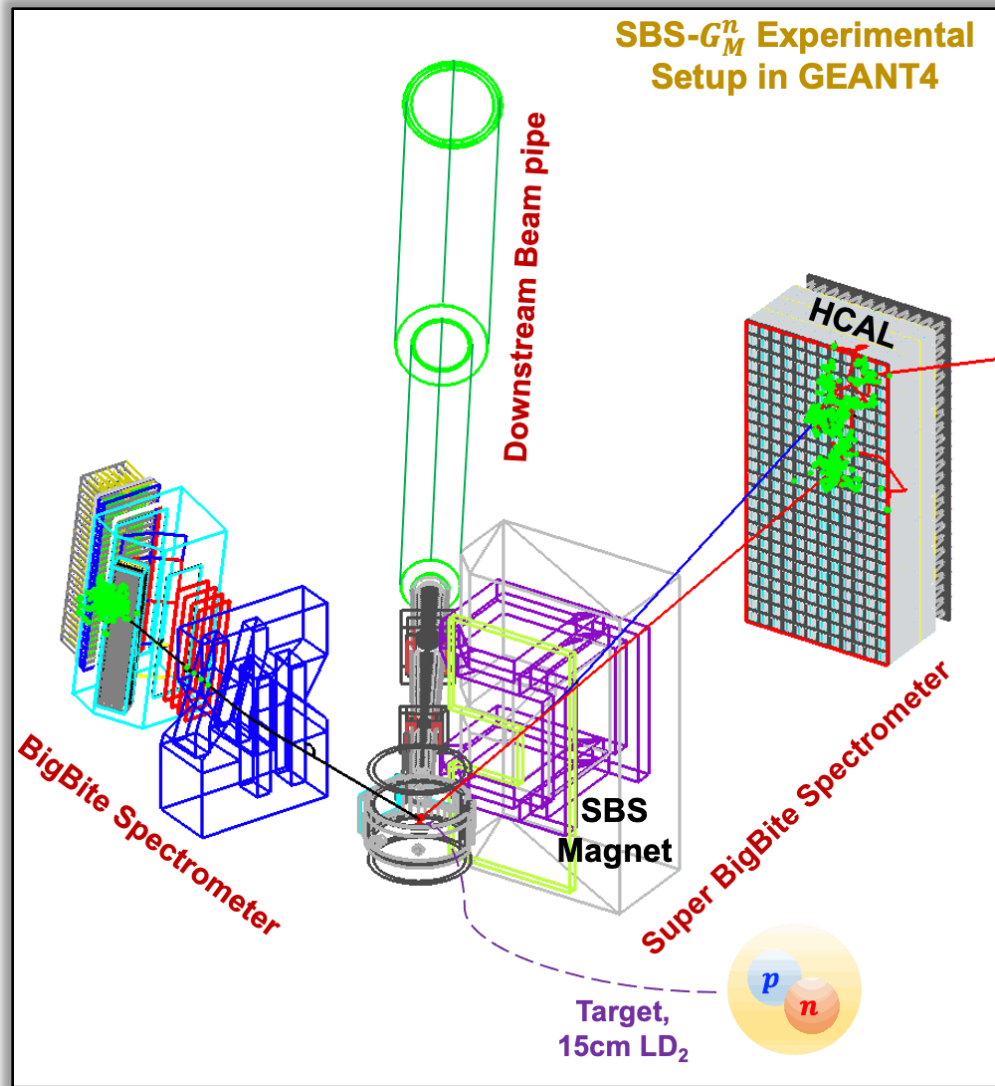
$$\begin{cases} \bullet Q^2 = -q^2 \\ \bullet \tau = Q^2/4M_N^2 \\ \bullet \epsilon = (1 + 2(1 + \tau)\tan^2(\theta_e/2))^{-1} \end{cases}$$



❖ Q^2 evolution of Sachs FFs reveal nucleon's internal structure.

† CLAS12 measured G_M^n up to $Q^2 = 10$ GeV^2 , results are yet to be published.

SBS-GMn Measurement Technique (“Ratio method”)



- Simultaneous detection of elastically scattered electrons and nucleons lets us use “ratio method”^[1], which is way less sensitive to systematic errors than other measurement techniques.

- 3 major steps to get G_M^n :

- 1 Extracting QE cross section ratio, R^{QE} , directly from the experiment:

$$R^{QE} = \frac{\frac{d\sigma}{d\Omega} | D(e, e' n)}{\frac{d\sigma}{d\Omega} | D(e, e' p)}$$

- 2 Apply nuclear and radiative corrections to obtain:

$$R = \frac{\frac{d\sigma}{d\Omega} | n(e, e')}{\frac{d\sigma}{d\Omega} | p(e, e')} \equiv \frac{\frac{\sigma_{Mott}}{1+\tau} (G_E^n^2 + \frac{\tau}{\epsilon} G_M^n^2)}{\frac{d\sigma}{d\Omega} | p(e, e')}$$

- 3 Finally,

$$G_M^n = - \left[\frac{\epsilon(1+\tau)}{\tau\sigma_{Mott}} \frac{d\sigma}{d\Omega} |_{p(e, e')} R - \frac{\epsilon}{\tau} G_E^n^2 \right]^{\frac{1}{2}}$$

[1] L. Durand, Phys. Rev. 115 1020 (1959).

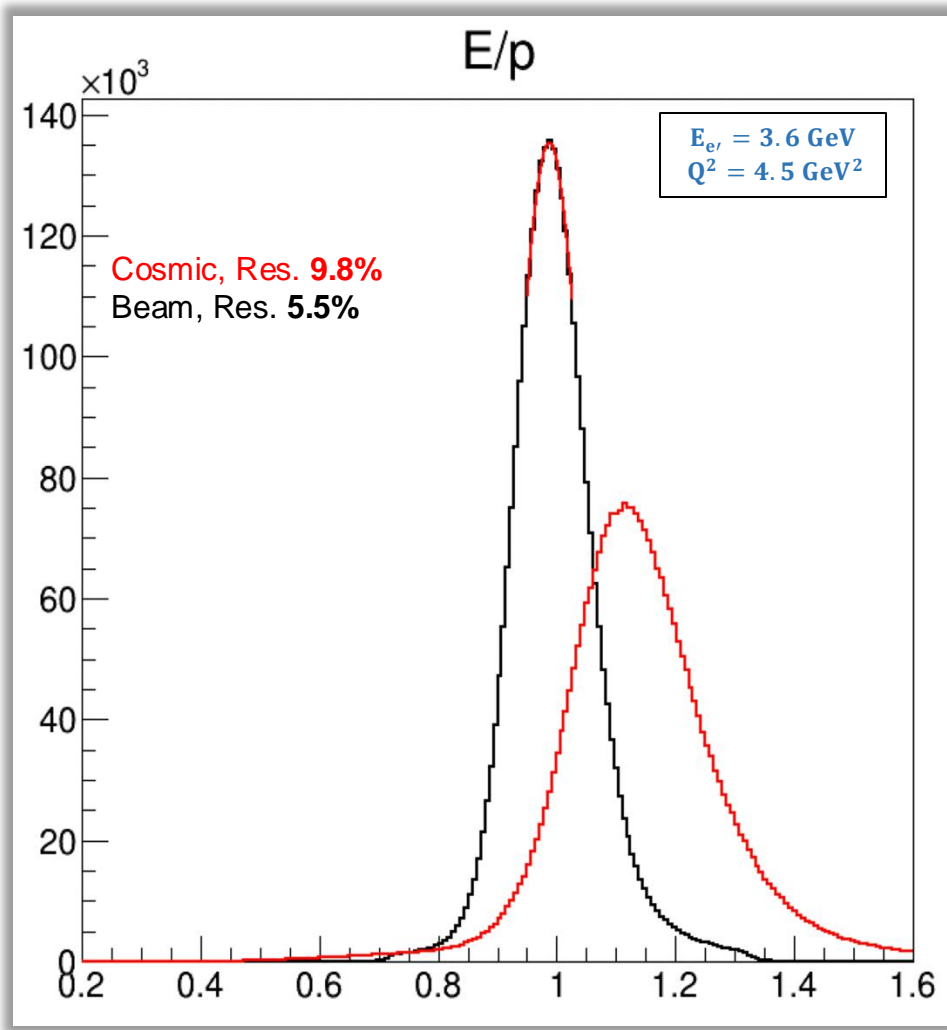
Kinematics of SBS-GMn

Table 1: Kinematics of SBS-GMn. Q^2 is the central Q^2 , E_{beam} is the beam energy, $\theta_{\text{BB}}(d_{\text{BB}})$ is the BigBite central angle (target-magnet distance), $\theta_{\text{SBS}}(d_{\text{SBS}})$ is the Super BigBite central angle (target-magnet distance), $\theta_{\text{HCAL}}(d_{\text{HCAL}})$ is the HCAL central angle (target-HCAL distance), ϵ is the longitudinal polarization of the virtual photon, $E_{e'}$ is the average scattered electron energy, and $E_{p'}$ is the average scattered proton energy.

SBS config.	Q^2 (GeV/c) ²	ϵ	E_{beam} (GeV)	θ_{BB} (deg)	d_{BB} (m)	θ_{SBS} (deg)	d_{SBS} (m)	θ_{HCAL} (deg)	d_{HCAL} (m)	$E_{e'}$ (GeV)	$E_{p'}$ (GeV)
4	3.0	0.72	3.73	36.0	1.79	31.9	2.25	31.9	11.0	2.12	2.4
9	4.5	0.51	4.03	49.0	1.55	22.5	2.25	22.0	11.0	1.63	3.2
8	4.5	0.80	5.98	26.5	1.97	29.9	2.25	29.4	11.0	3.58	3.2
14	7.4	0.46	5.97	46.5	1.85	17.3	2.25	17.3	14.0	2.00	4.8
7	9.9	0.50	7.91	40.0	1.85	16.1	2.25	16.0	14.0	2.66	6.1
11	13.6	0.41	9.86	42.0	1.55	13.3	2.25	13.3	14.5	2.67	8.1

- We took data at five different spectrometer configurations for high- Q^2 G_M^n extraction.
- Data taken with **SBS-8** configuration in combination with SBS-9 dataset will be used for Rosenbluth separation to shed some light on the two-photon exchange (TPE) contribution in the elastic $e-n$ scattering. **Goal of a short and parasitic but very interesting experiment, SBS-nTPE (E12-20-010).**

Detector Performance Highlights



▪ BigBite Spectrometer:

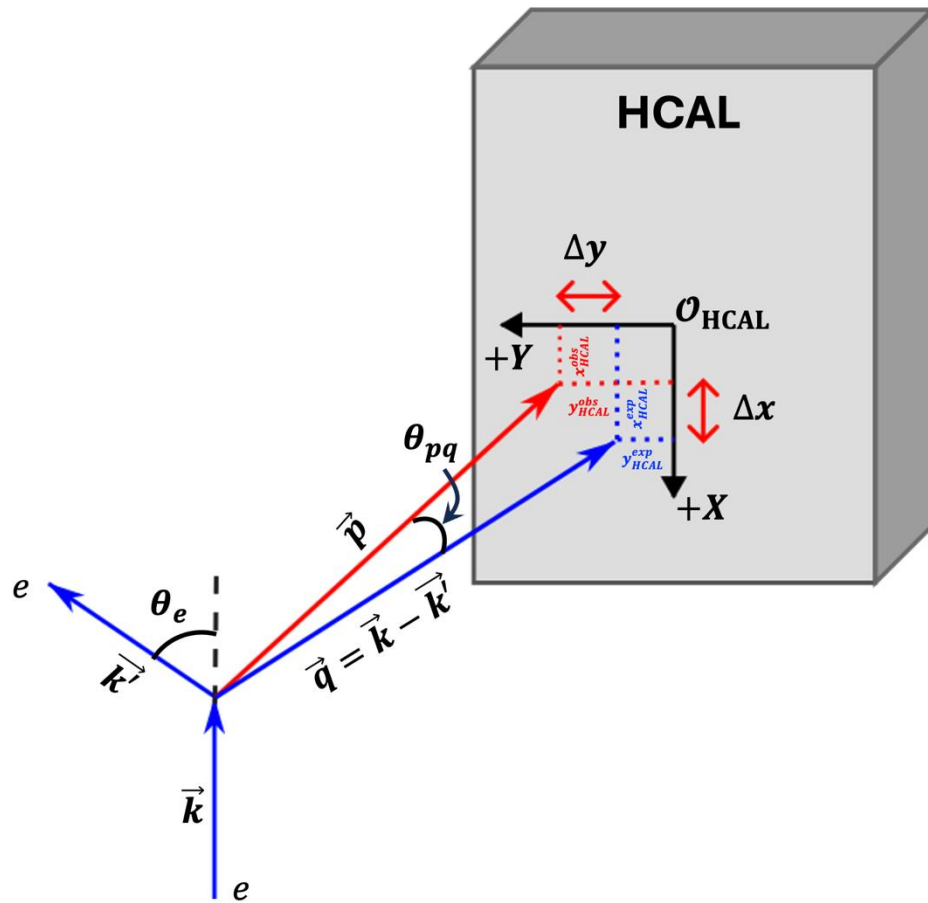
- Momentum resolution $\left(\frac{\sigma_p}{p}\right)$: **1 – 1.5%**
- Angular resolution (in-plane & out-of-plane): **1 – 2 mrad**
- Vertex resolution: **2 – 6 mm**
- BBCAL energy resolution $\left(\frac{\sigma_E}{E}\right)$: **5.4 – 6.2%**

▪ Super BigBite Spectrometer:

- Hadron Calorimeter (HCAL):
 - Time Resolution: **1.2 – 1.3 ns**
 - Position Resolution: **5 – 6 cm**

- Brief Overview
- **Physics Analysis Methodology**
- Extraction of Experimental Observable
- Systematic Uncertainty Quantification
- Preliminary Results
- Summary and outlook

Physics Analysis Methods – Introducing HCAL Δx and Δy

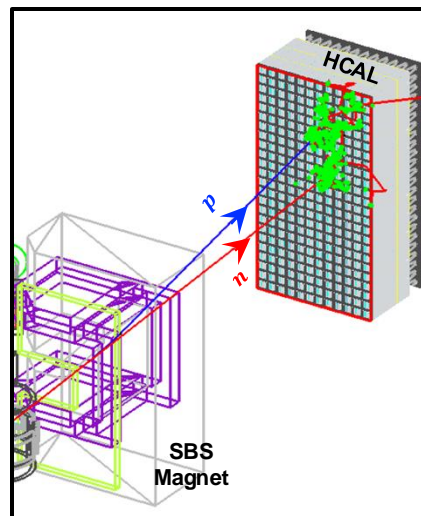
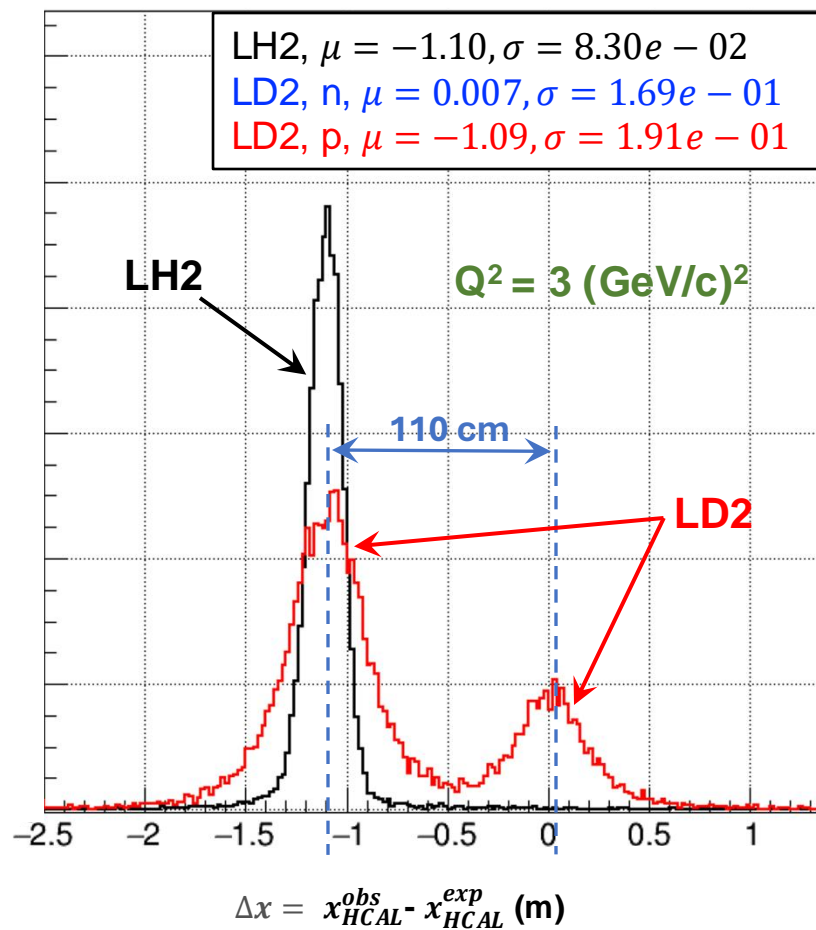


- **Definition of Δx :** The difference between the observed (x_{HCAL}^{obs}) and expected (x_{HCAL}^{exp}) nucleon position on HCAL in the vertical (dispersive) direction.
- **Definition of Δy :** The difference between the observed (y_{HCAL}^{obs}) and expected (y_{HCAL}^{exp}) nucleon position on HCAL in the horizontal (non-dispersive) direction.

Figure 1: A conceptual and exaggerated diagram introducing HCAL Δx and Δy variables. **NOTE:** The presence of the SBS magnet has been **ignored** here.

Physics Analysis Methods – Introducing HCAL Δx and Δy

❖ Introducing HCAL Δx plot:



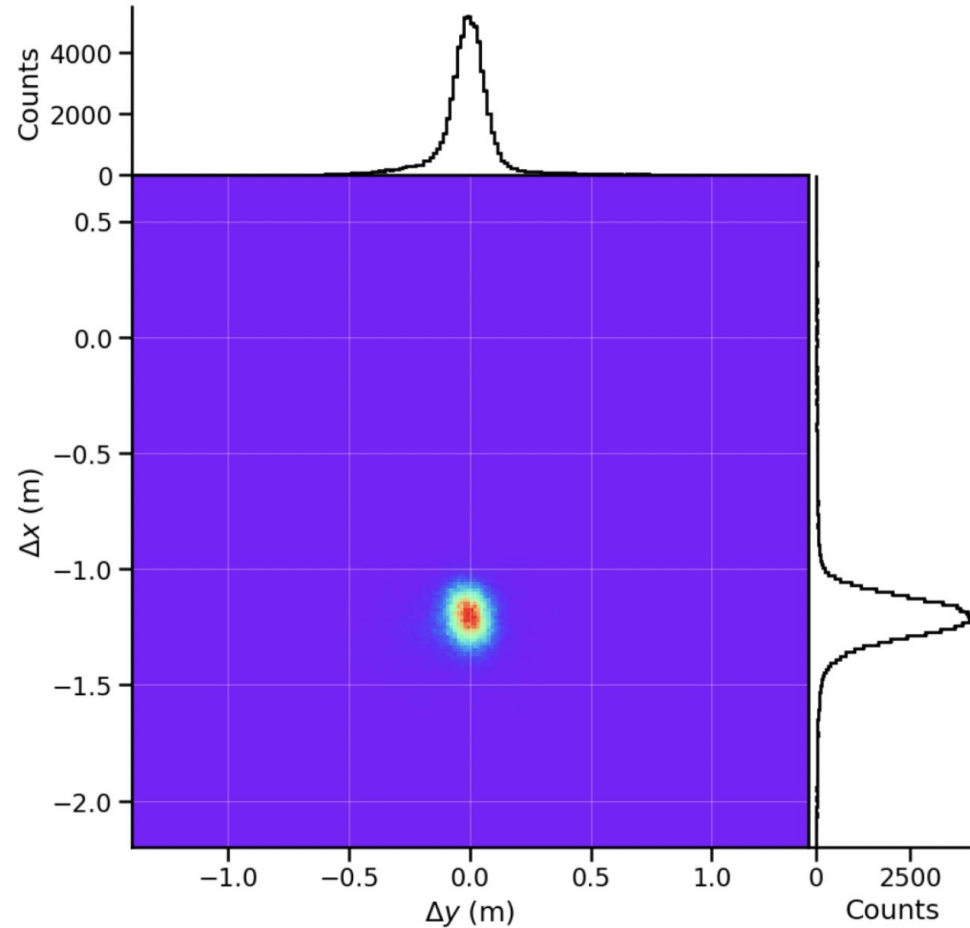
❖ From the Δx plot we can extract $D(e, e'n)$ & $D(e, e'p)$ counts and then form the ratio.

$$R^{QE} = \frac{\frac{d\sigma}{d\Omega} | D(e, e'n)}{\frac{d\sigma}{d\Omega} | D(e, e'p)}$$

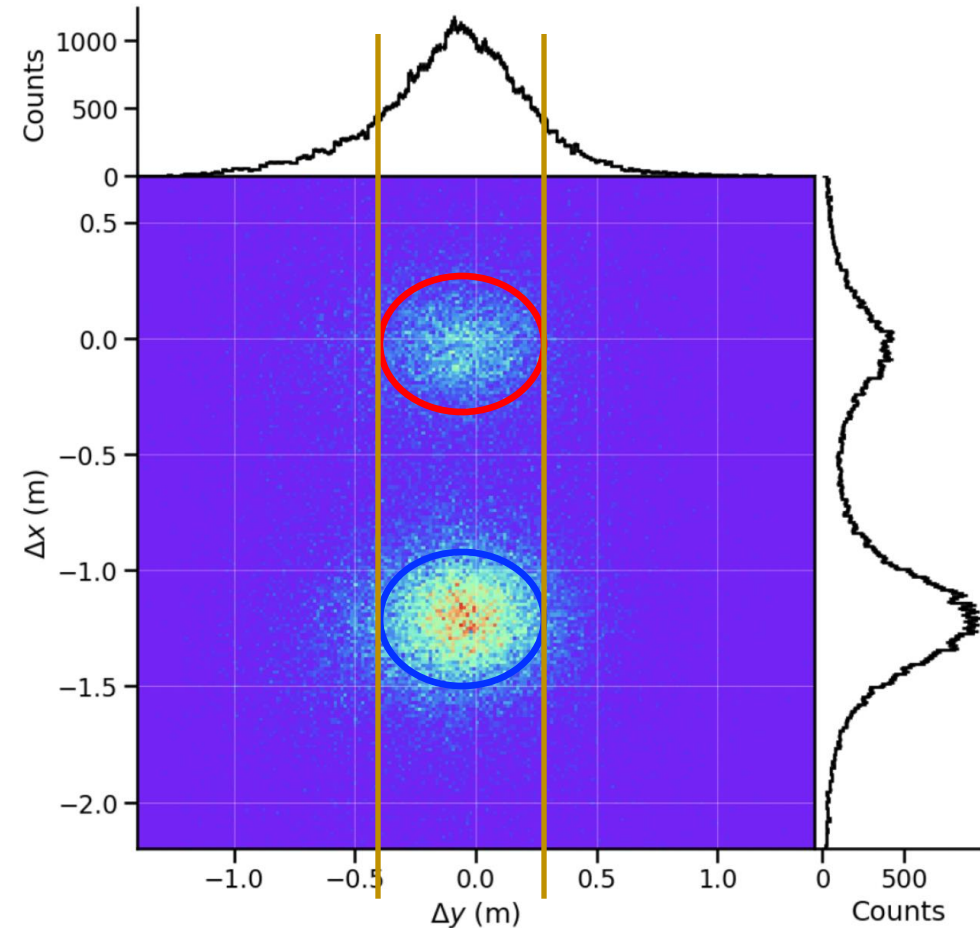
HCAL Δx and Δy Correlation

$Q^2 = 3 \text{ (GeV/c)}^2$, SBS 50% Field

Elastic Spot (LH₂ Data)



Quasi-Elastic Spots (LD₂ Data)



List of Analysis Cuts

- **Good e Track Selection Cuts:**

- 1. Track Quality

- 1. No. of GEM layers with hits > 3
 - 2. $|(vertex)_z| < 0.08$ m
 - 3. E/p
 - 4. BB optics validity

- 2. PID Cuts

- 1. Pre-Shower energy > 0.2 GeV
 - 2. GRINCH cluster size > 2

- **Good HCAL Event Selection:**

- 1. HCAL energy
 - 2. HCAL active area
 - 3. Shower-HCAL ADC coincidence time

- **Quasi-Elastic Event Selection Cuts:**

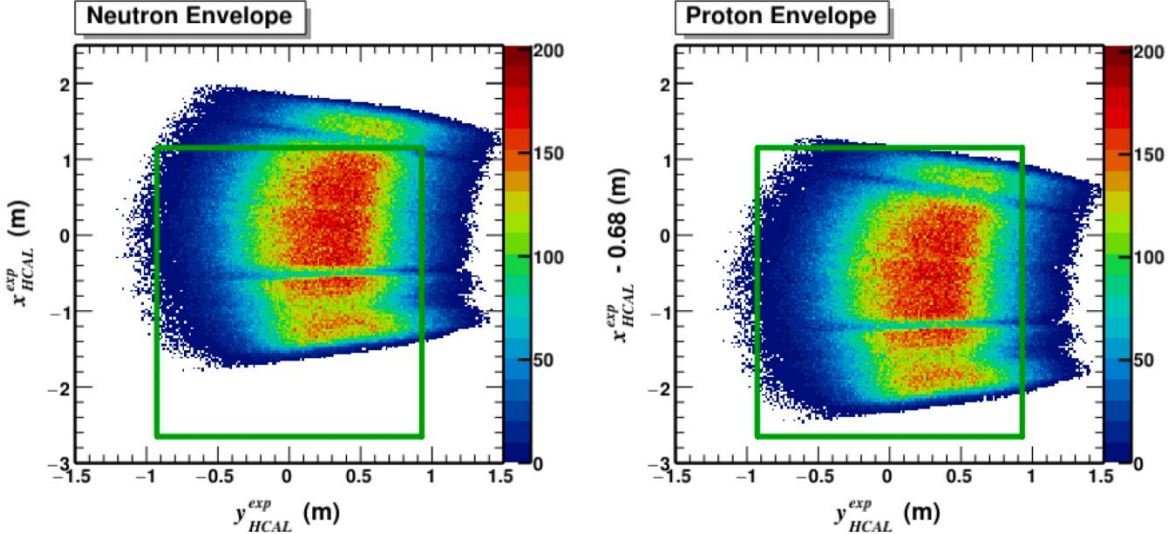
- 1. W^2 cut
 - 2. Δx - Δy correlation / θ_{pq} cut
 - 3. Δy cut

- **Fiducial / Acceptance Matching Cut**

Effect of Fiducial Cut

$Q^2 = 3 \text{ (GeV/c)}^2$

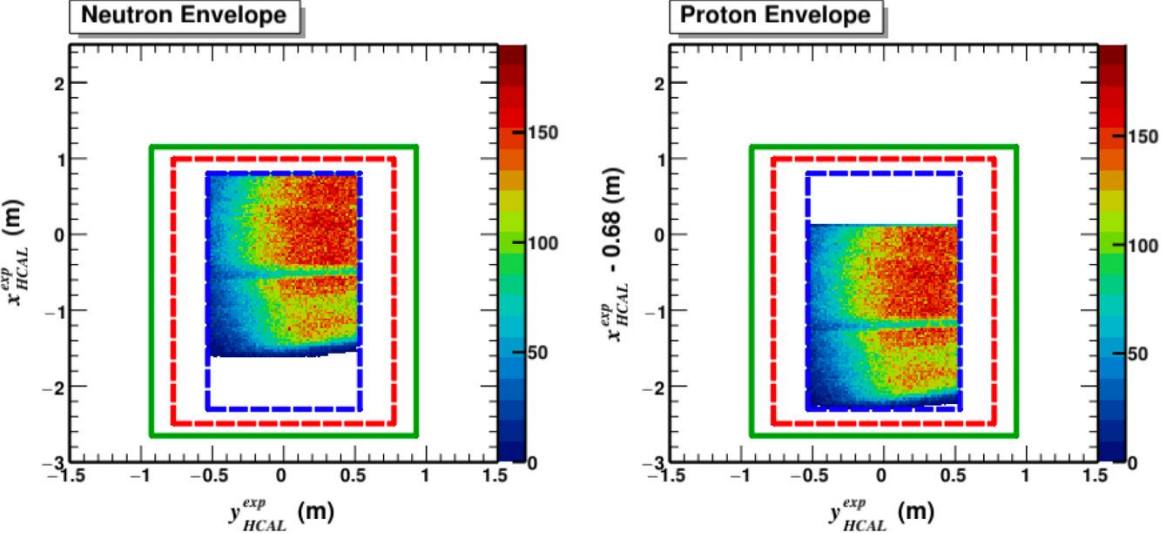
No Fiducial Cut



--- Top of HCAL ---

- HCAL Physical Boundary
- - - HCAL Active Area
- - - HCAL Safety Margin

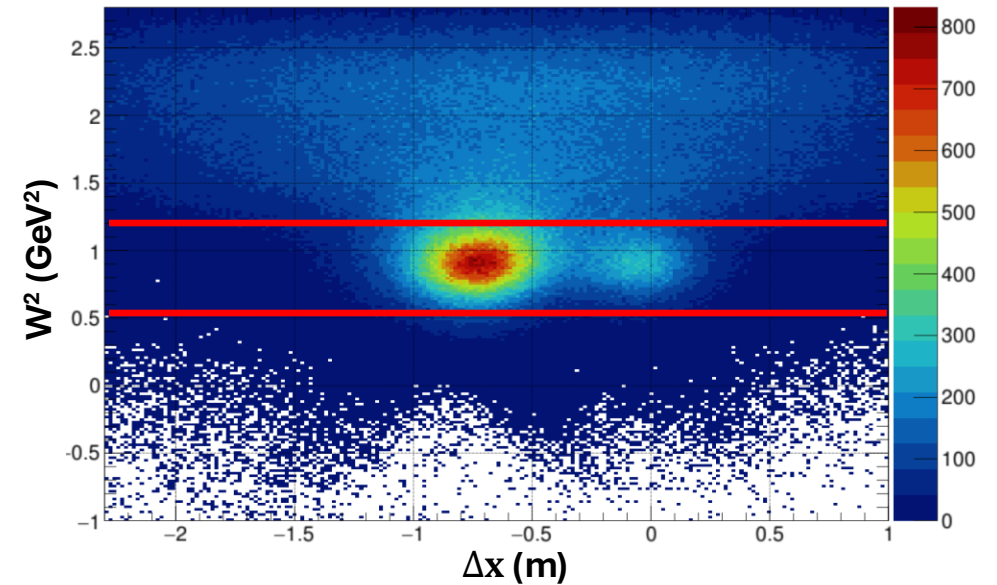
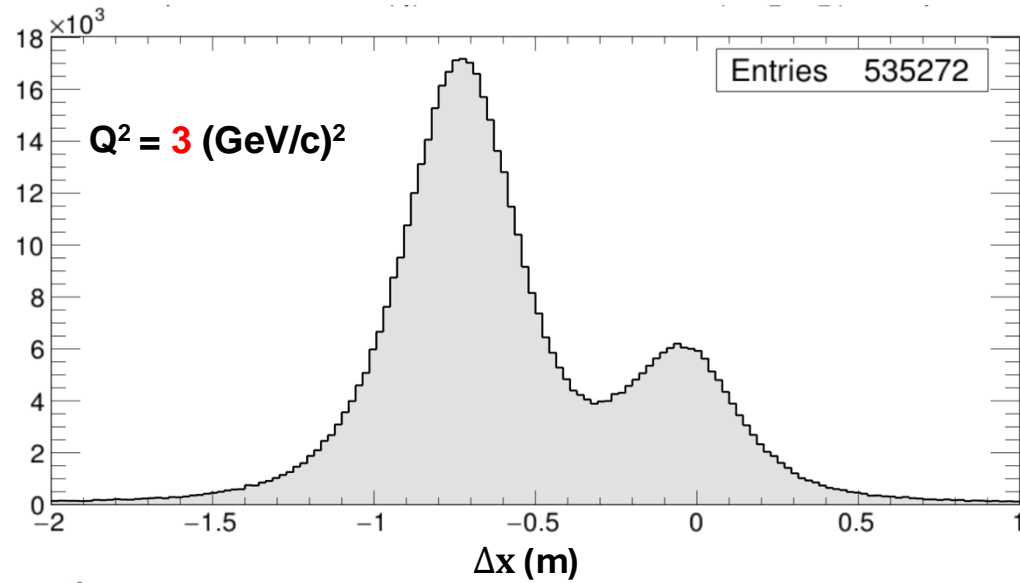
With Fiducial Cut



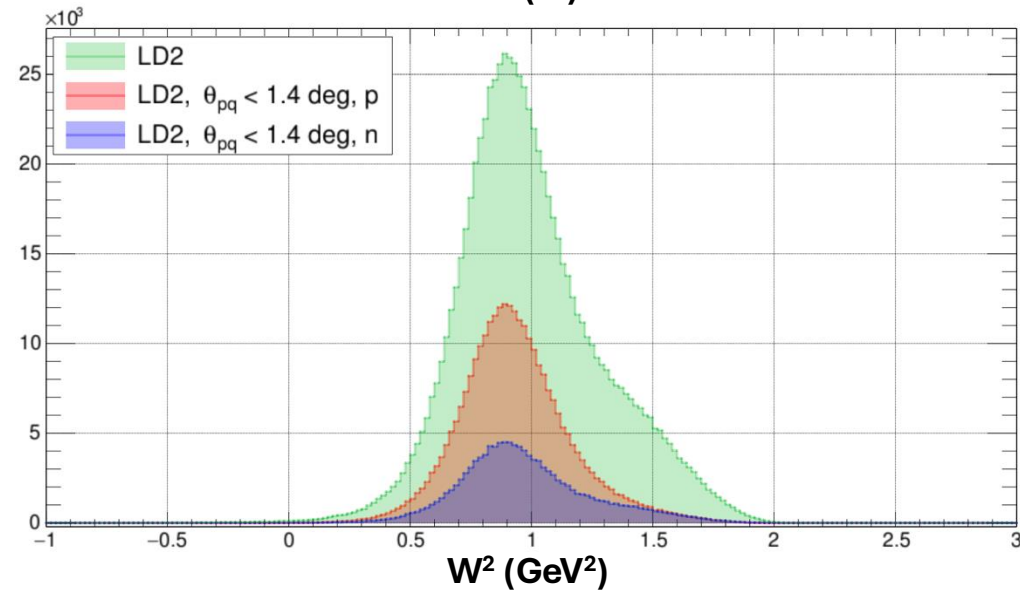
--- Top of HCAL ---

❖ Fiducial cut effectively matches the acceptances for $D(e,e'n)$ and $D(e,e'p)$ events, essential to reduce systematic error in the ratio.

Quasi-Elastic (QE) Event Selection: $Q^2 = 3 \text{ (GeV/c)}^2$



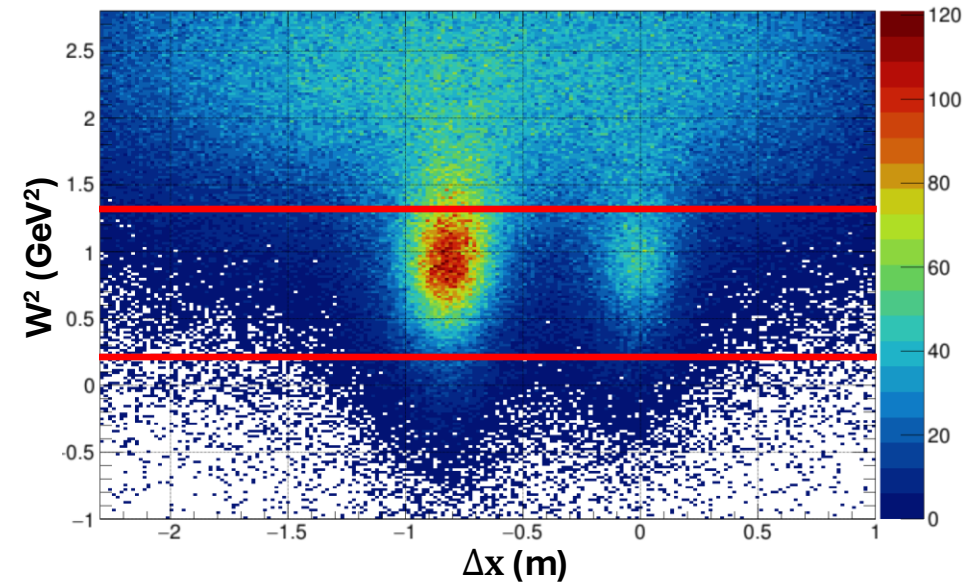
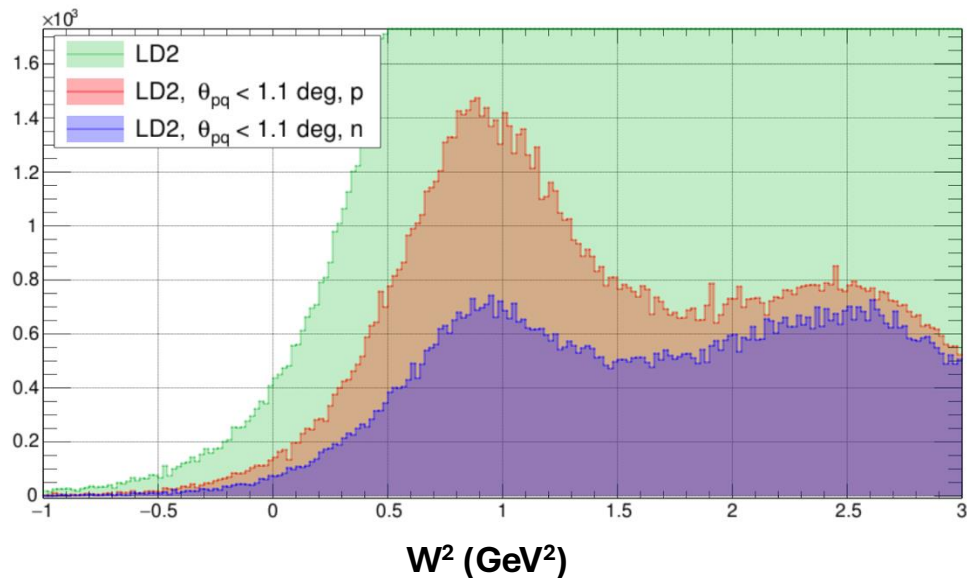
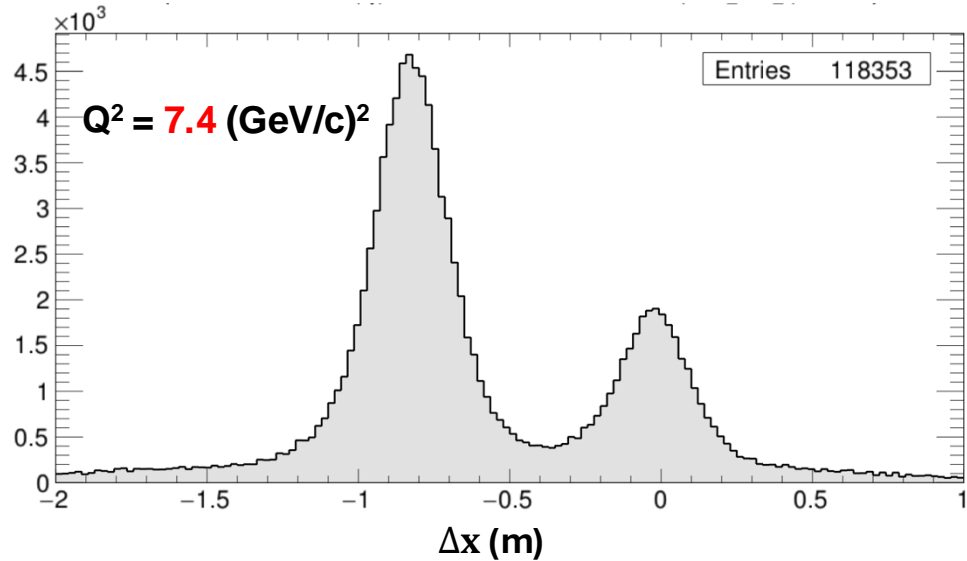
Figures: HCAL Δx (Top Left), W^2 vs HCAL Δx (Top Right), W^2 (Bottom Left)



List of cuts:

- Primary cuts to choose good electron tracks.
- Fiducial cuts
- Coincidence time cut
- $0.25 \leq W^2 \leq 1.2 \text{ GeV}^2$ (HCAL Δx plot)
- $|\Delta y| < 0.3 \text{ m}$ (HCAL Δx plot)
- $\theta_{pq} < 1.4^\circ$ with **p** hypothesis (W^2 plot)
- $\theta_{pq} < 1.4^\circ$ with **n** hypothesis (W^2 plot)

QE Event Selection: $Q^2 = 7.4 \text{ (GeV/c)}^2$

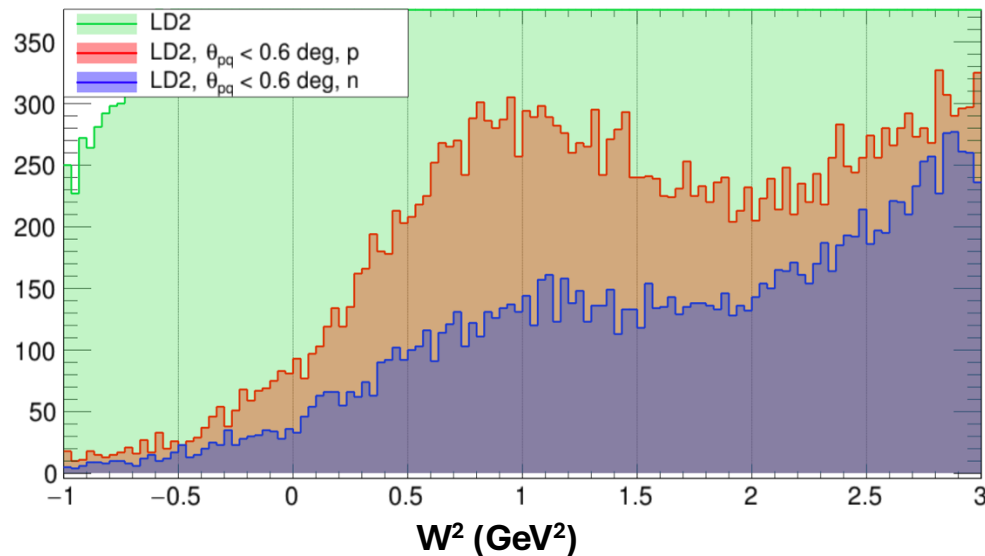
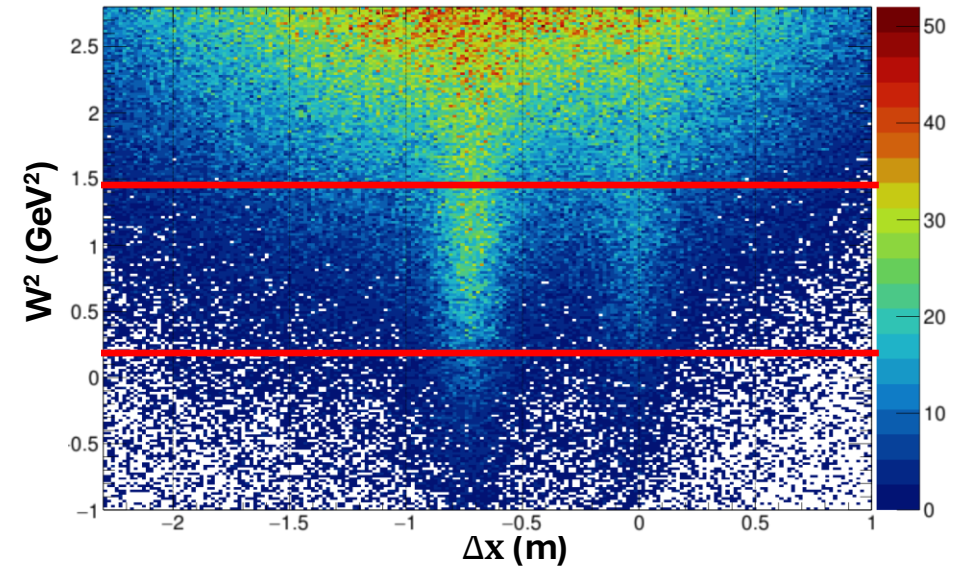
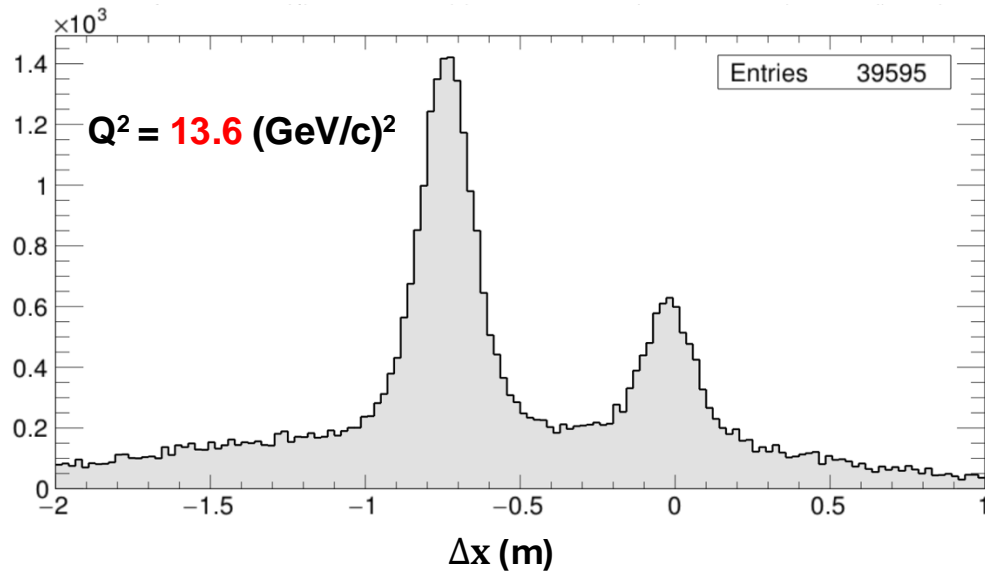


Figures: HCAL Δx (Top Left), W^2 vs HCAL Δx (Top Right), W^2 (Bottom Left)

List of cuts:

- Primary cuts to choose good electron tracks.
- Fiducial cuts
- Coincidence time cut
- $0.5 \leq W^2 \leq 1.15 \text{ GeV}^2$ (HCAL Δx plot)
- $|\Delta y| < 0.3 \text{ m}$ (HCAL Δx plot)
- $\theta_{pq} < 1.1^\circ$ with **p** hypothesis (W^2 plot)
- $\theta_{pq} < 1.1^\circ$ with **n** hypothesis (W^2 plot)

QE Event Selection: $Q^2 = 13.6 \text{ (GeV/c)}^2$



Figures: HCAL Δx (Top Left), W^2 vs HCAL Δx (Top Right), W^2 (Bottom Left)

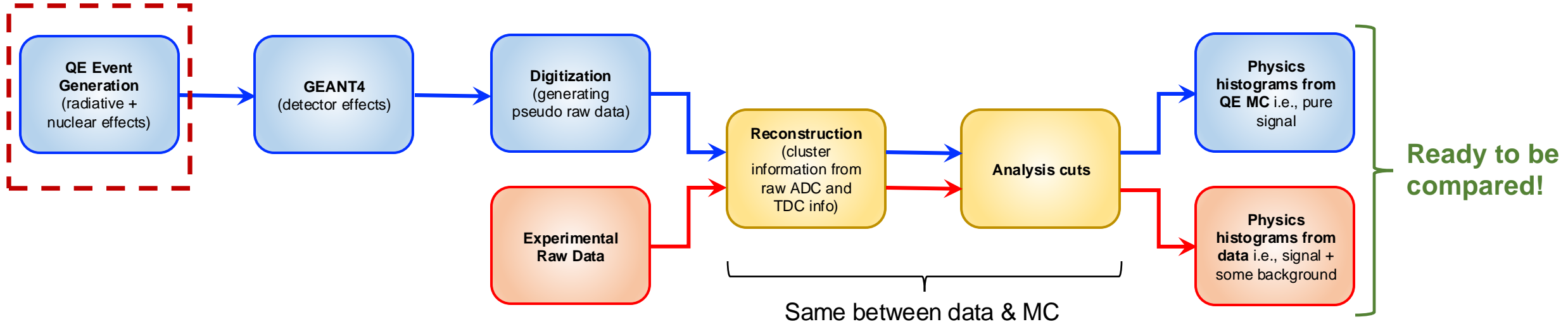
List of cuts:

- Primary cuts to choose good electron tracks.
- Fiducial cuts
- Coincidence time cut
- $0.16 \leq W^2 \leq 1.44 \text{ GeV}^2$ (HCAL Δx plot)
- $|\Delta y| < 0.25 \text{ m}$ (HCAL Δx plot)
- $\theta_{pq} < 0.6^\circ$ with **p** hypothesis (W^2 plot)
- $\theta_{pq} < 0.6^\circ$ with **n** hypothesis (W^2 plot)

- Brief Overview
- Physics Analysis Methodology
- **Extraction of Experimental Observable**
- Systematic Uncertainty Quantification
- Preliminary Results
- Summary and outlook

Analysis Flow for Data/MC Comparison

❖ Steps to perform realistic data/MC comparisons:

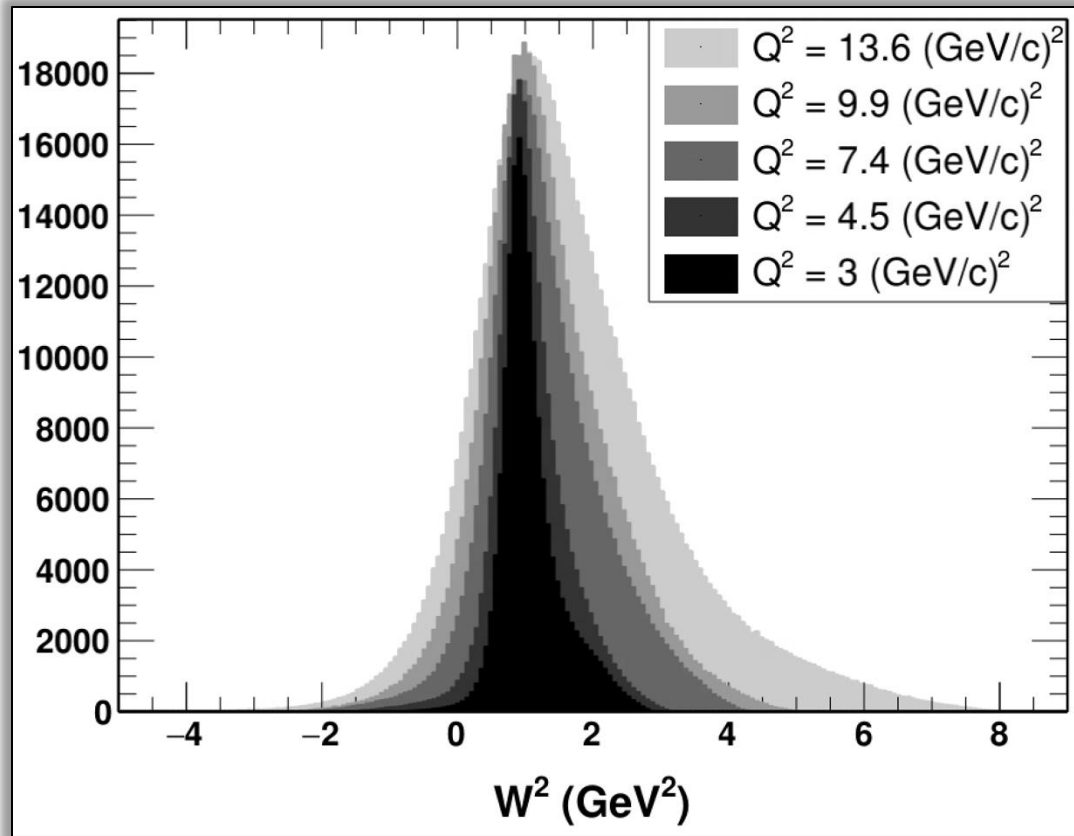


❖ Key components of the quasi-elastic event generator:

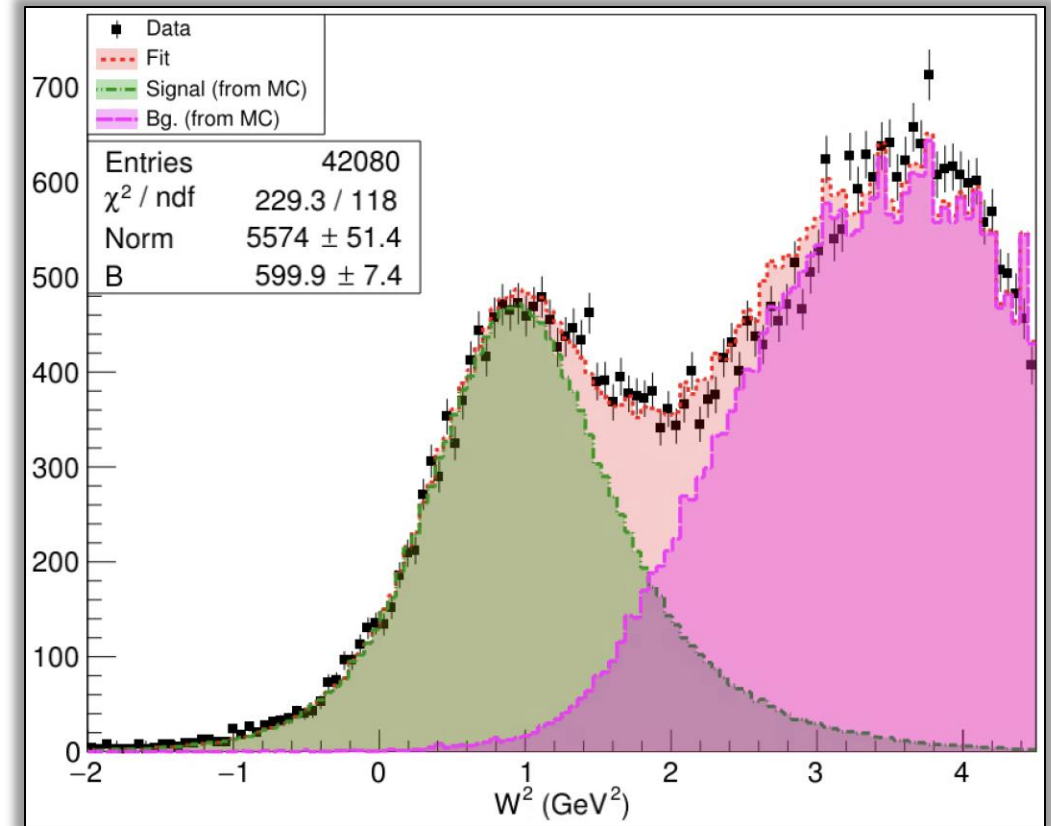
- D_2 wave function based on Bonn potential.
- Missing momentum (p_{miss}) extends up to 1.2 GeV.
- Off shell scattering cross section is based on T. de Forest model.
- Radiative correction is based on the work of R. Ent *et al.*

Qualitative Data/MC Comparison of W^2 Distribution

Quasi-Elastic MC (SIMC)



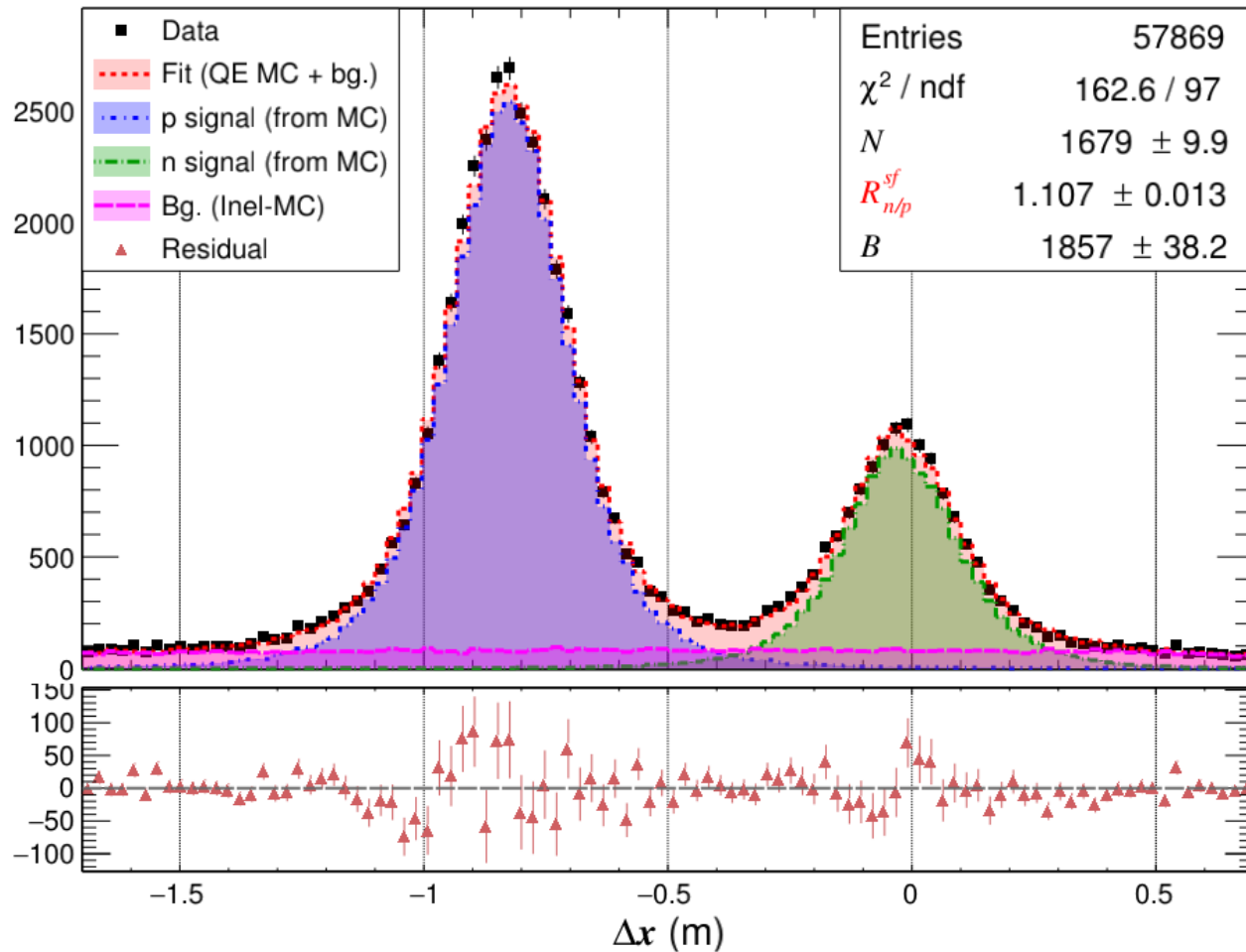
Data/MC Comparison at $Q^2 = 13.6$ (GeV/c)²



- The kinematic broadening of the W^2 distribution with increasing Q^2 is accurately produced in the MC.
- Qualitative data/MC comparison looks encouraging even for the most challenging kinematics.

Data/MC Fit to Δx Dist.: $Q^2 = 7.4 \text{ (GeV/c)}^2$

$Q^2 = 7.4 \text{ (GeV/c)}^2$



❖ Fit equation:

$$simu_i = \mathcal{N} * (p_histo_i + R_{n/p}^{sf} * n_histo_i) + B * bg_histo_i$$

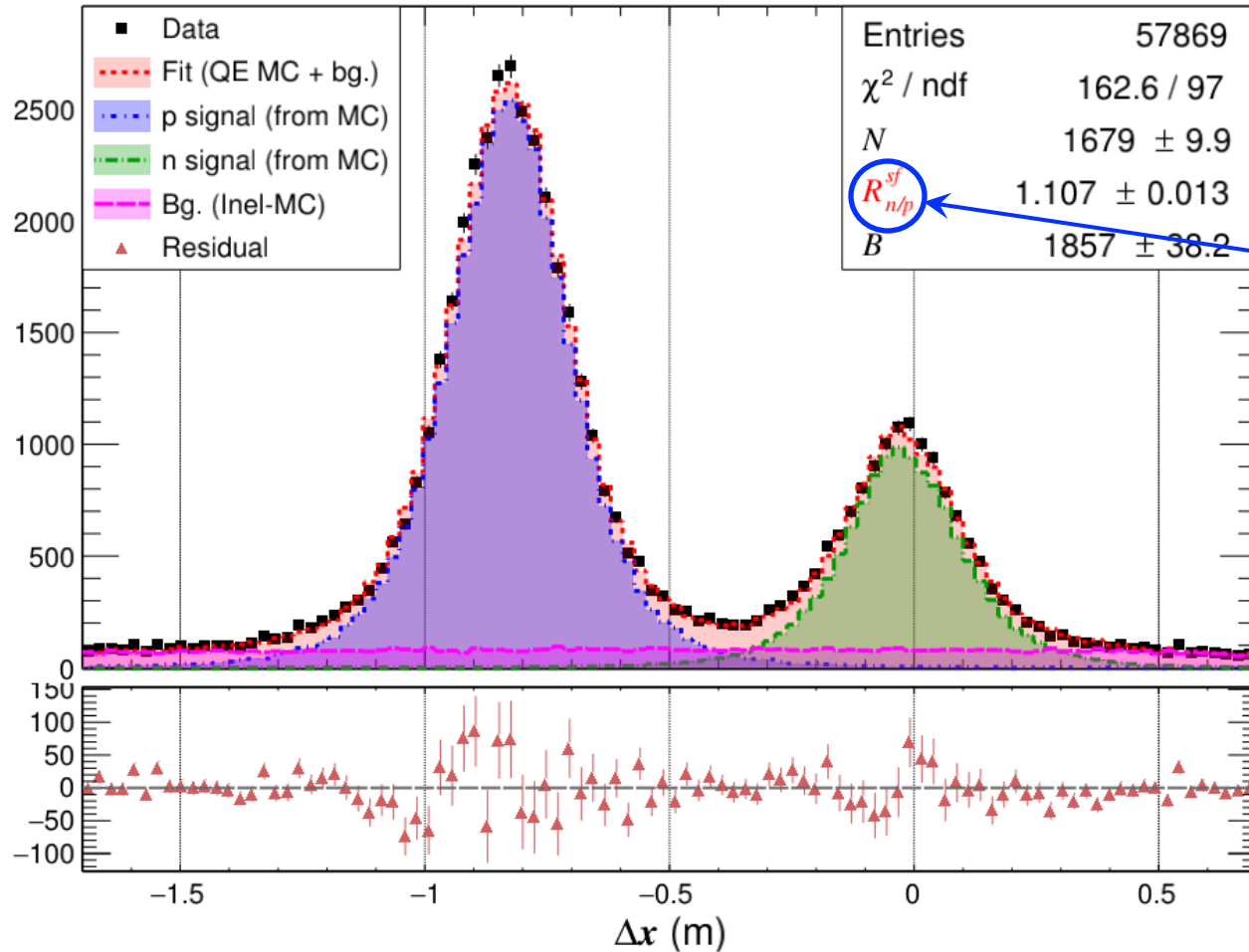
❖ Fit parameters:

1. N – Overall proton normalization.
2. $R_{n/p}^{sf}$ – Relative n/p normalization.
3. B – Overall background normalization.

❖ Agreement of fit looks good in the entire range.

Method of GMn Extraction from Data/MC Fit

$Q^2 = 7.4 \text{ (GeV/c)}^2$



❖ Assumption:

- Simulation accurately represents nuclear, radiative, and detector effects that are present in data.

❖ Interpretation:

- The fit parameter $R_{n/p}^{sf}$, i.e. the relative n/p normalization, is a measure of the discrepancy in the neutron to proton Born cross section ratio between simulation and data.

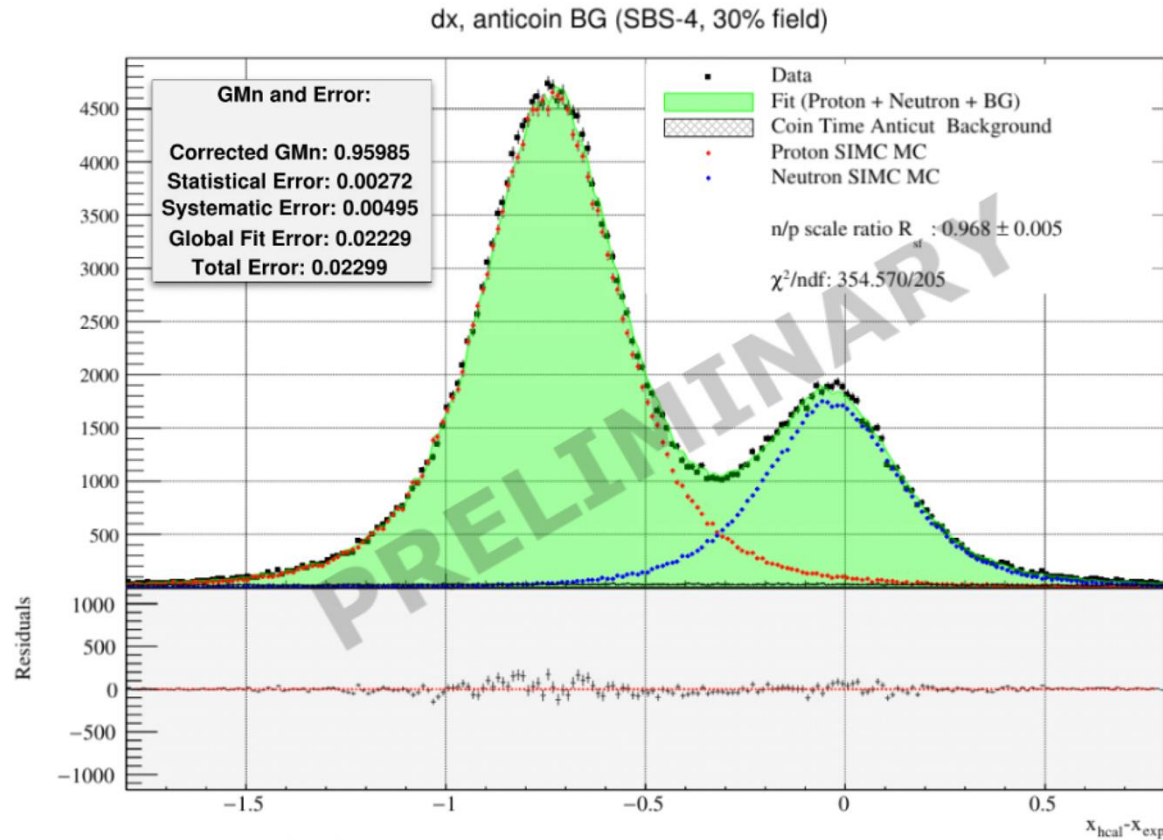
❖ GMn extraction:

$$R = \frac{\frac{d\sigma}{d\Omega} \Big|_n(e,e')}{\frac{d\sigma}{d\Omega} \Big|_p(e,e')} = R_{n/p}^{sf} * R_{MC}$$

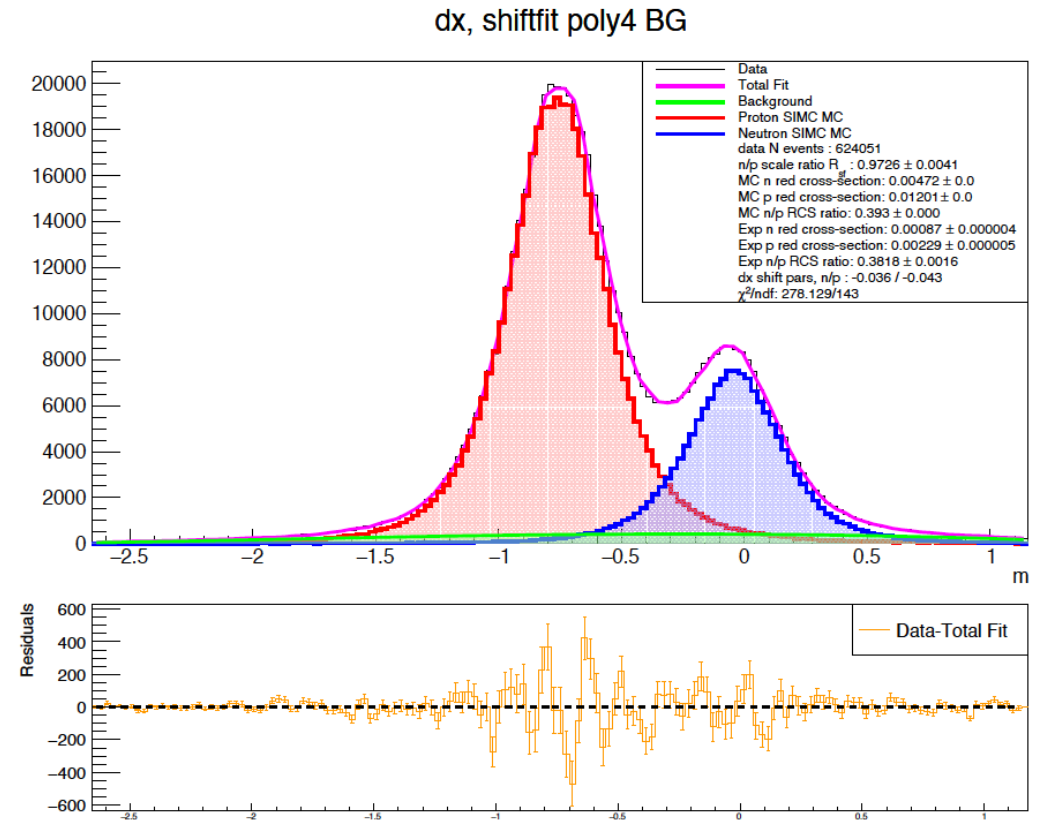
$$\Rightarrow G_M^n = - \left[\frac{\epsilon(1 + \tau)}{\tau\sigma_{Mott}} \frac{d\sigma}{d\Omega} \Big|_p(e,e') R - \frac{\epsilon}{\tau} G_E^m{}^2 \right]^{\frac{1}{2}}$$

Data/MC Fit to Δx Dist.: $Q^2 = 3 \text{ (GeV/c)}^2$

$Q^2 = 3 \text{ (GeV/c)}^2$



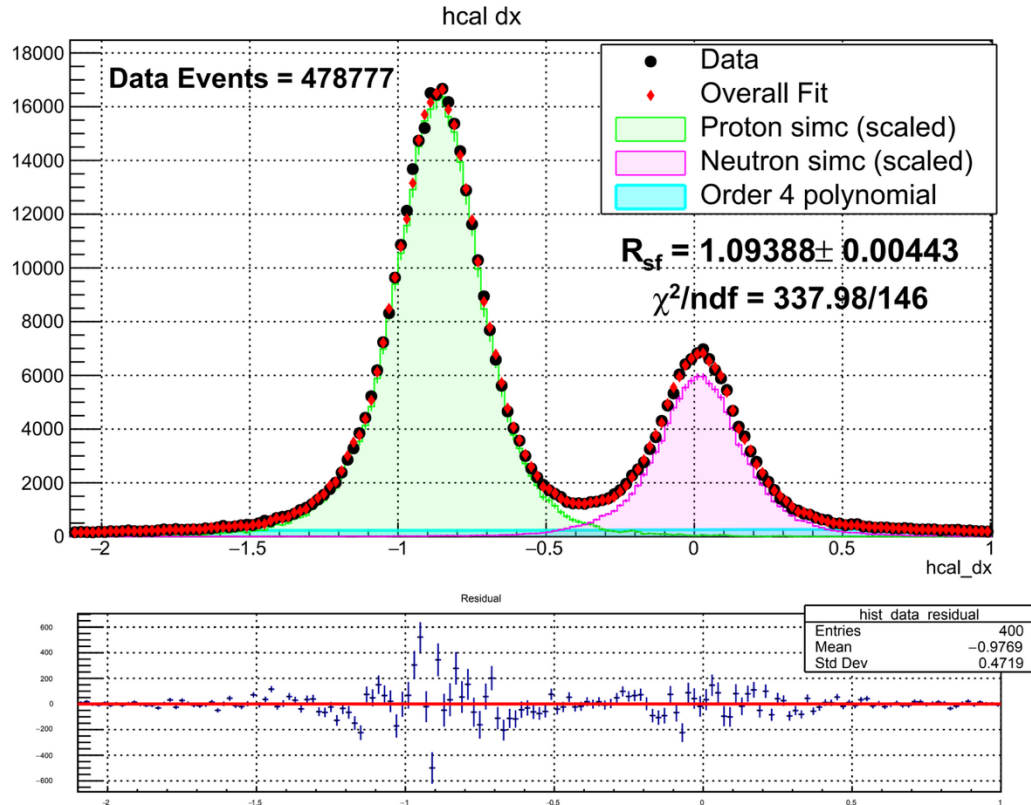
Credit: Sebastian Seeds



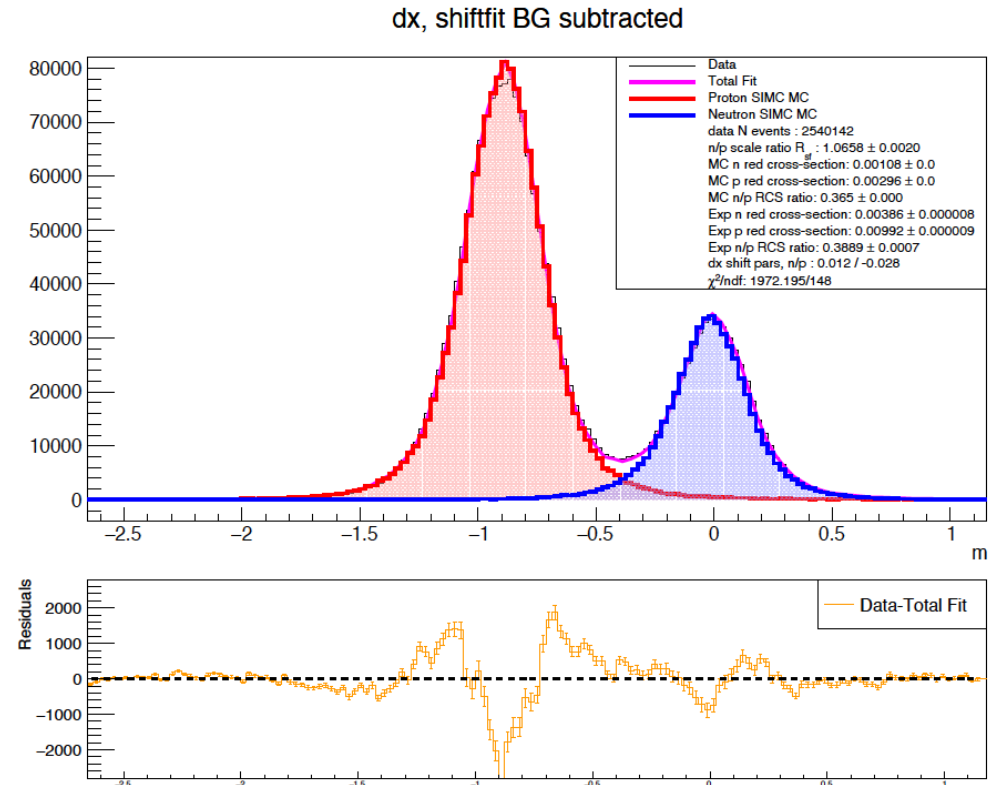
Credit: Zeke Wertz

Data/MC Fit to Δx Dist.: $Q^2 = 3 \text{ (GeV/c)}^2$

$Q^2 = 4.5 \text{ (GeV/c)}^2$



Credit: Maria Satnik

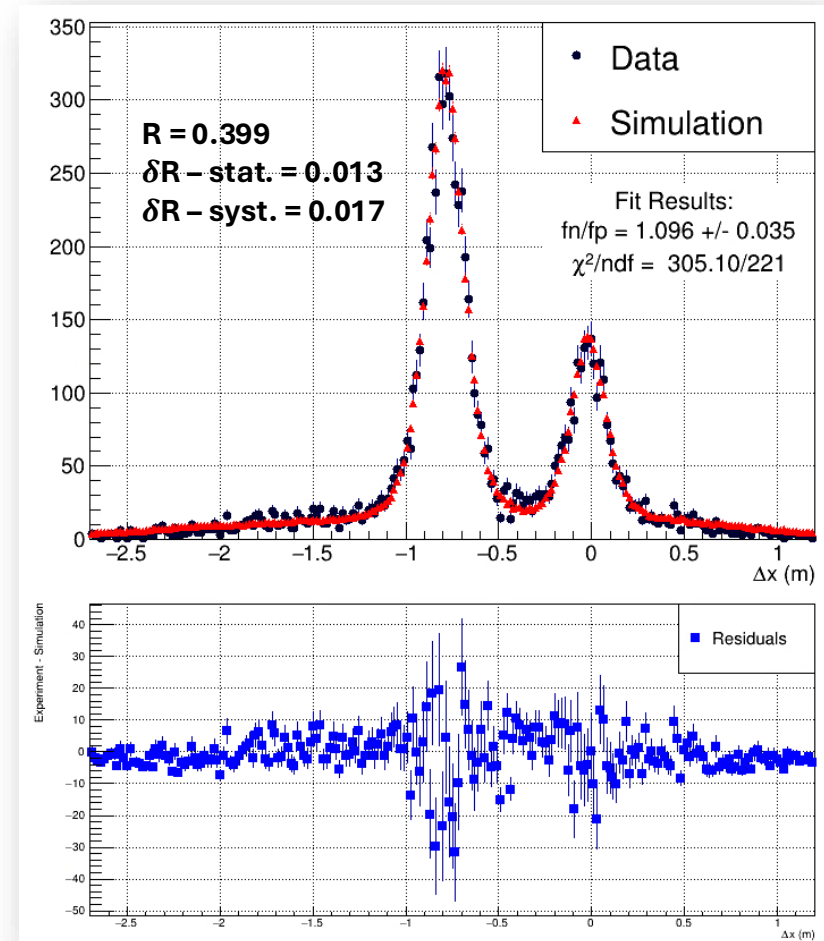
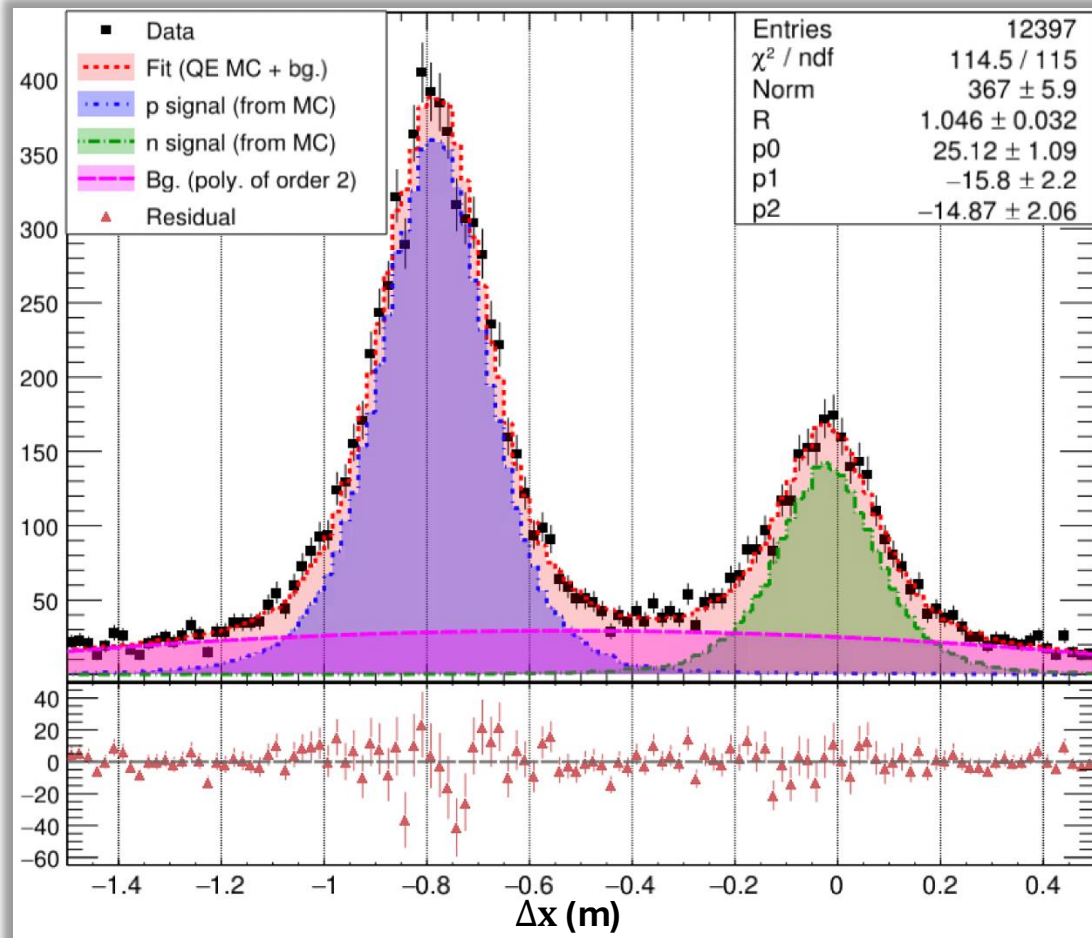


Credit: Zeke Wertz

Data/MC Fit to Δx Dist.: $Q^2 = 9.9 \text{ (GeV/c)}^2$

$Q^2 = 9.9 \text{ (GeV/c)}^2$

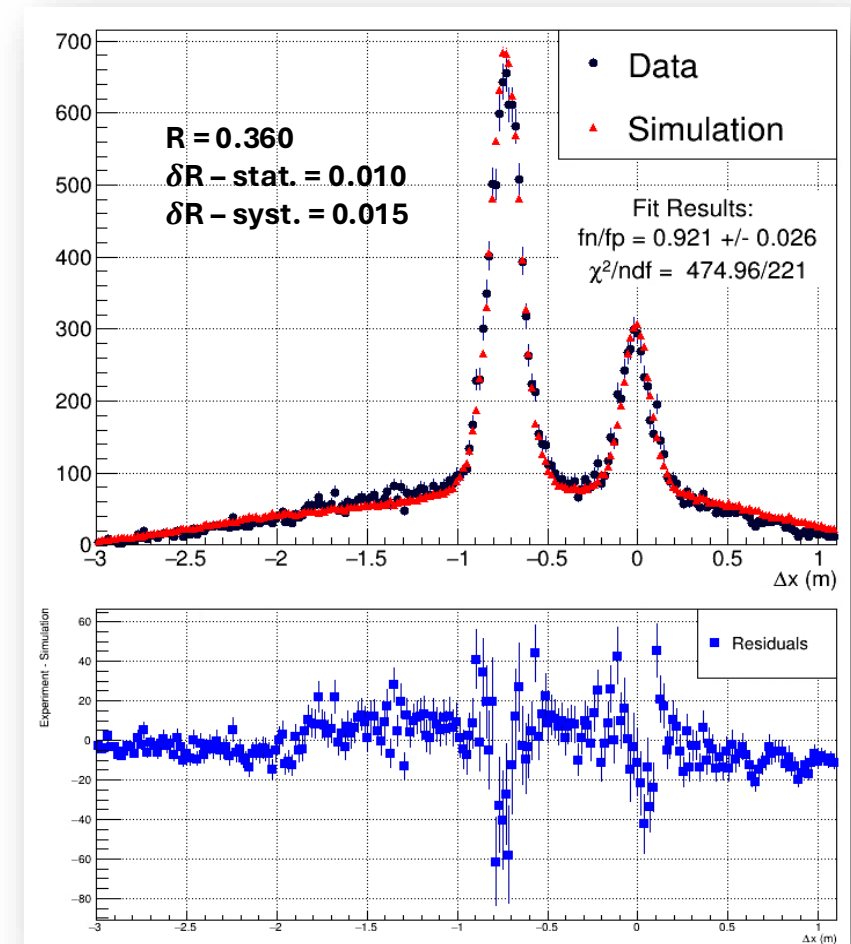
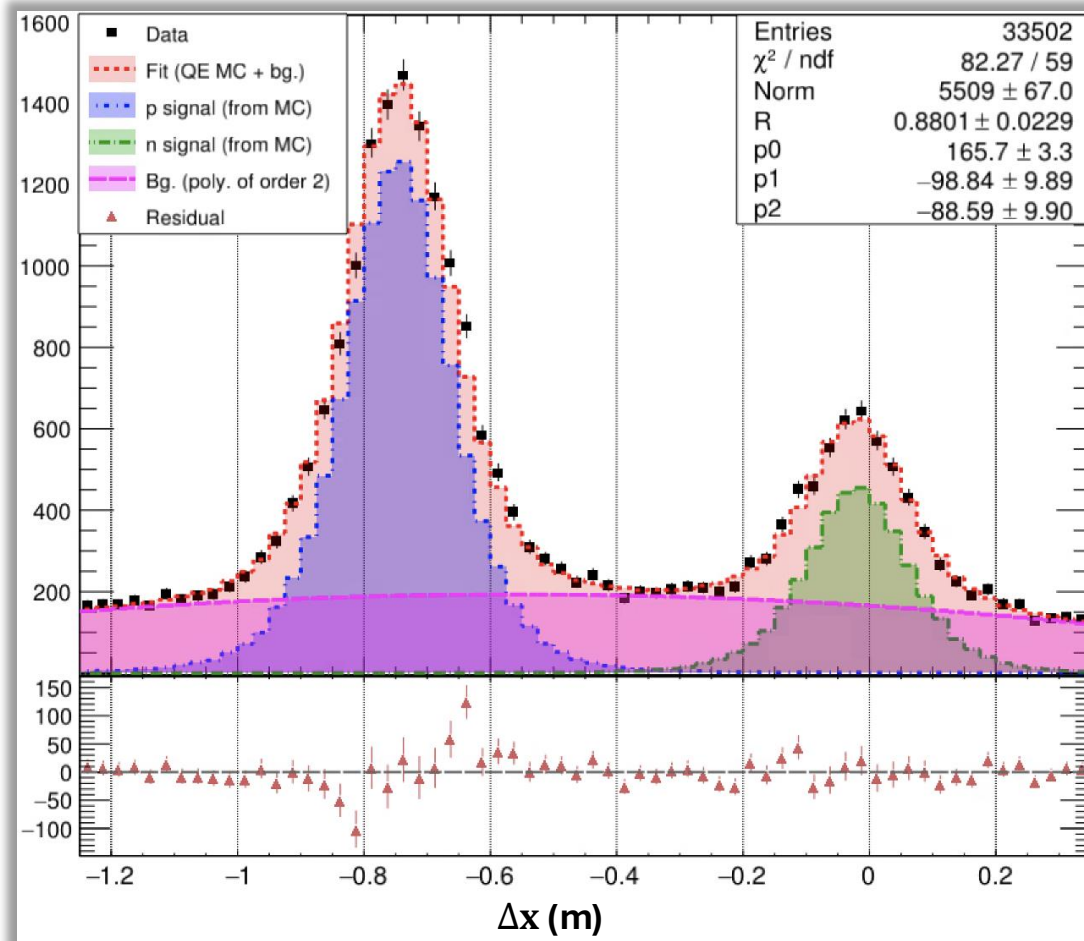
Credit: **Anuruddha Rathnayake**



Data/MC Fit to Δx Dist.: $Q^2 = 13.6 \text{ (GeV/c)}^2$

$Q^2 = 13.6 \text{ (GeV/c)}^2$

Credit: **Anuruddha Rathnayake**



Cut Optimization

Goal: Obtain an optimized set of cuts that yields best possible signal to background and does not affect $D(e,e'n)$ and $D(e,e'p)$ events differently, essential to ensure unbiased $R_{n/p}^{sf}$ extraction.

Approach:

- Study the stability of the experimental observables, R^{QE} and/or $R_{n/p}^{sf}$, as a function of the cut variables in the region of interest.
- Choose the cut range that excludes the region of instability.

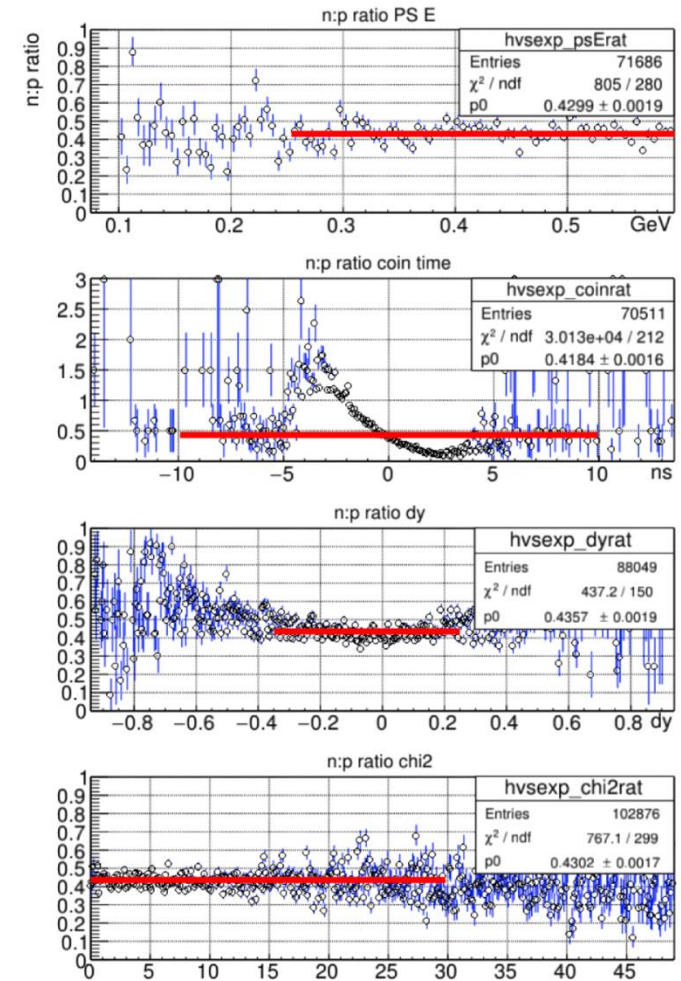
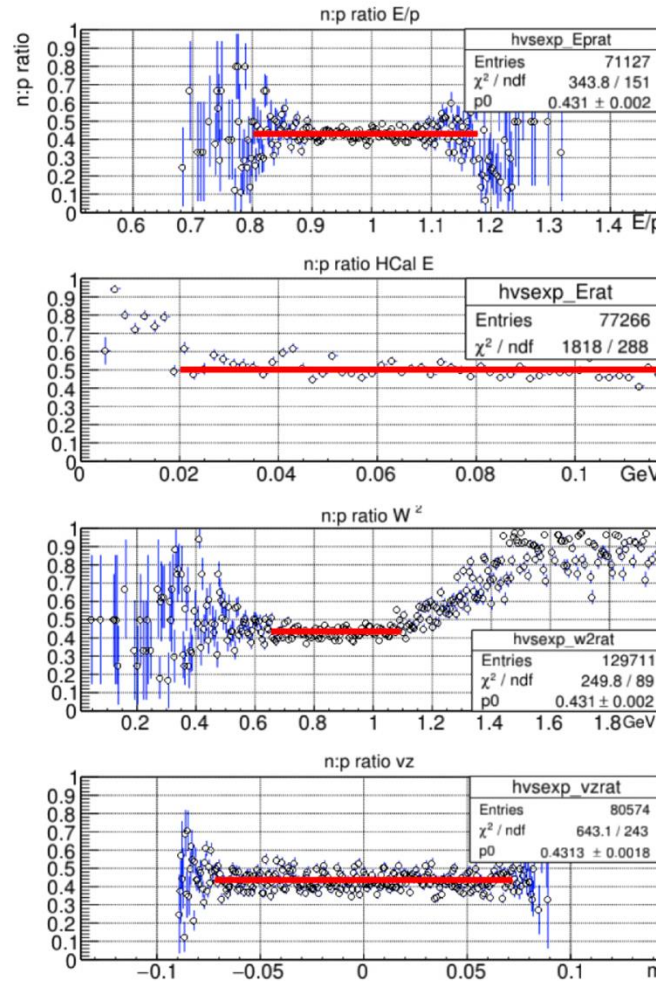
Stability of R^{QE} vs. Cut Variables

$Q^2 = 3 \text{ (GeV/c)}^2$

n:p ratio = R^{QE}

$$R^{QE} = \frac{\frac{d\sigma}{d\Omega} \big|_{D(e,e'n)}}{\frac{d\sigma}{d\Omega} \big|_{D(e,e'p)}}$$

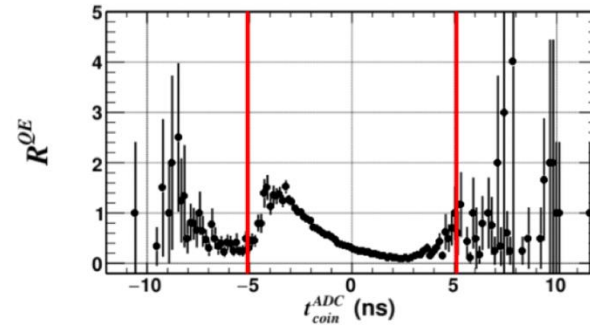
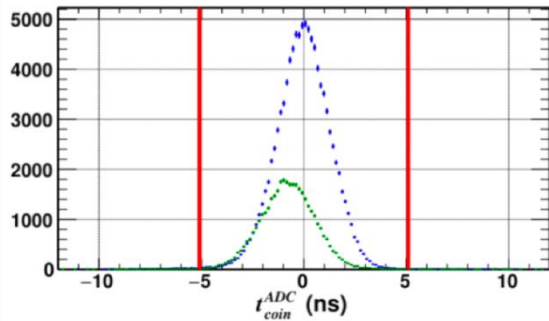
Plots Credit: **Sebastian Seeds**



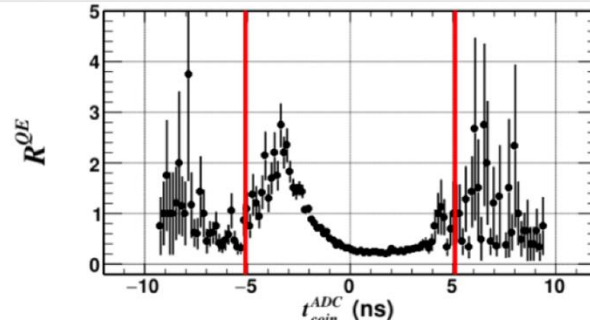
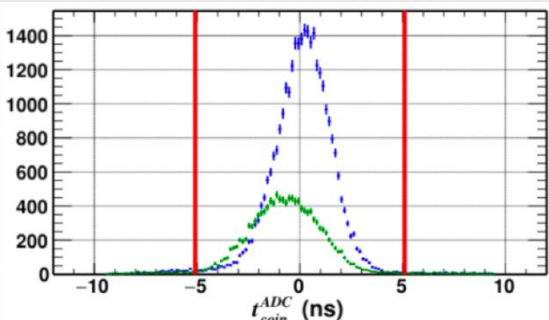
- R^{QE} is stable in the region of interest except for Shower-HCAL ADC coincidence time.

Stability of R^{QE} vs. Shower-HCAL ADC Coin Time

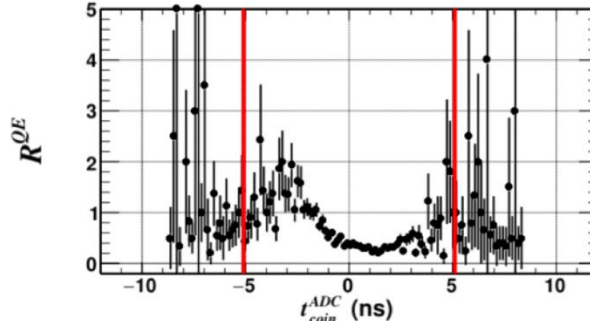
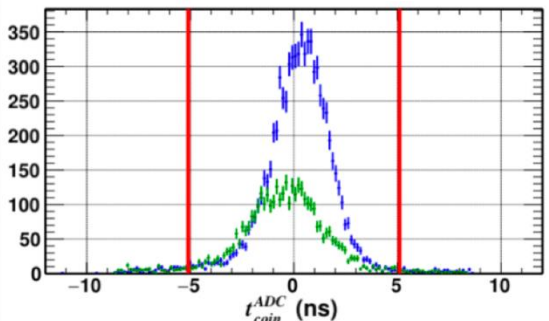
$Q^2 = 3 \text{ (GeV/c)}^2$



$Q^2 = 7.4 \text{ (GeV/c)}^2$



$Q^2 = 13.6 \text{ (GeV/c)}^2$



- The instability in R^{QE} arises from the misalignment of coincidence time (t_{coin}^{ADC}) peak associated to **proton** and **neutron** events.
- Similar trend is observed for all kinematics.
- Situation should improve with better calibration. Efforts are ongoing.
- At the moment, the strategy is to make the cut range wide enough to avoid the region of instability.

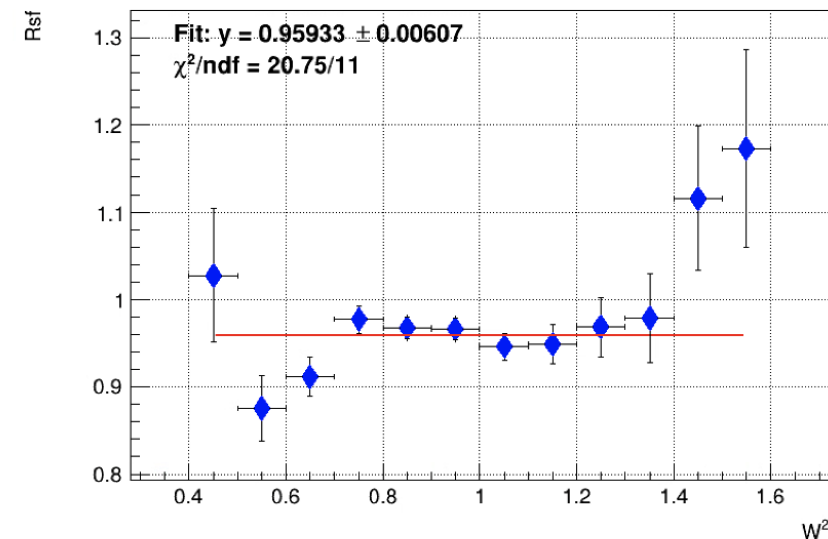
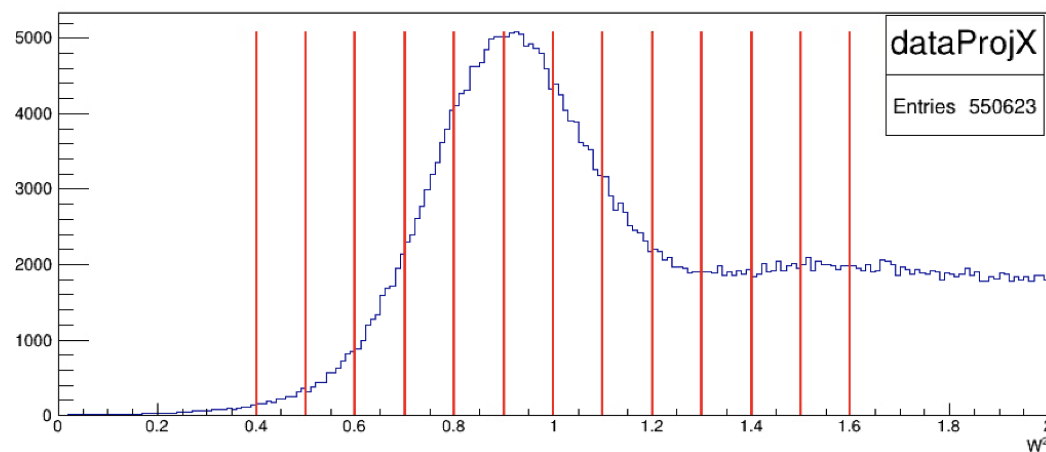
Stability of $R_{n/p}^{sf}$ vs. Cut Variables

$Q^2 = 3 \text{ (GeV/c)}^2$

Slide Credit: **Maria Satnik**

Cut Stability Study Using Slices and Data-MC comparison

- Create slices over a given variable (say W^2) for data and Monte Carlo
- Perform a data-MC comparison over each slice
- See how R_{sf} varies



Summary of Optimized Set of Cuts

From My Independent Analysis

Table II: Summary of the optimized set of cuts used for the final analysis. Cut variables marked with * are applied only to data.

Cut Variable	Q^2 (ϵ)				
	3 (0.72)	4.5 (0.51)	7.4 (0.46)	9.9 (0.50)	13.6 (0.41)
N_{hit}^{GEM}	> 3	> 3	> 3	> 3	> 2
Track χ^2/NDF	< 15	< 15	< 15	< 15	< 15
v_z (cm)	(-7, 7)	(-7, 7)	(-7.5, 6.5)	(-7, 7)	(-7.5, 7.5)
x_{BB} (cm)	-12, 30	(-20, 35)	(-25, 25)	(-20, 30)	(-25, 25)
y_{BB} (cm)	(-9, 9)	(-9, 10)	(-9, 9)	(-9, 9)	(-9, 9)
E_{PS} (GeV)	> 0.2	> 0.2	> 0.2	> 0.2	> 0.2
E_{BBCAL}/p	(0.8, 1.2)	(0.7, 1.3)	(0.85, 1.15)	(0.8, 1.2)	(0.8, 1.2)
$Size_{clus}^{GRINCH}$ *	-	> 2	-	-	-
E_{HCAL} (GeV)	> 0.025	0.1	> 0.12	> 0.2	> 0.2
$ t_{coin}^{ADC} $ (ns) *	< 5.1	< 5.1	< 5.1	< 5.1	< 5.1
W^2 (GeV ²)	(0.5, 1.2)	(0.25, 1.2)	(0.3, 1.3)	(0.3, 1.3)	(0.2, 1.45)
Δy (m)	(-0.3, 0.3)	(-0.3, 0.3)	(-0.3, 0.3)	(-0.3, 0.3)	(-0.25, 0.25)
$[x_{HCAL}^{exp}]^{(p,n)}$ (m)	(-2.22, 0.72)	(-2.28, 0.78)	(-2.32, 0.82)	(-2.36, 0.86)	(-2.36, 0.86)
y_{HCAL}^{exp} (m)	(-0.5, 0.5)	(-0.5, 0.5)	(-0.5, 0.5)	(-0.5, 0.5)	(-0.5, 0.5)

- Summary of optimized set of cuts evaluated for all GMn kinematics.
- Final $R_{n/p}^{sf}$ values are extracted based on these cuts.

- Brief Overview
- Physics Analysis Methodology
- Extraction of Experimental Observable
- **Systematic Uncertainty Quantification**
- Preliminary Results
- Summary and outlook

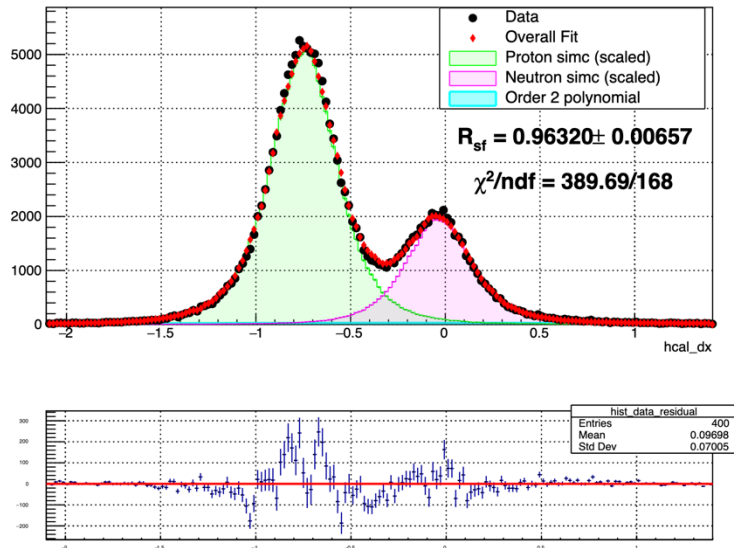
Source of Systematic Uncertainty

- Inelastic Contamination
- Cut Stability
- HCAL Nucleon Detection Efficiency (NDE)

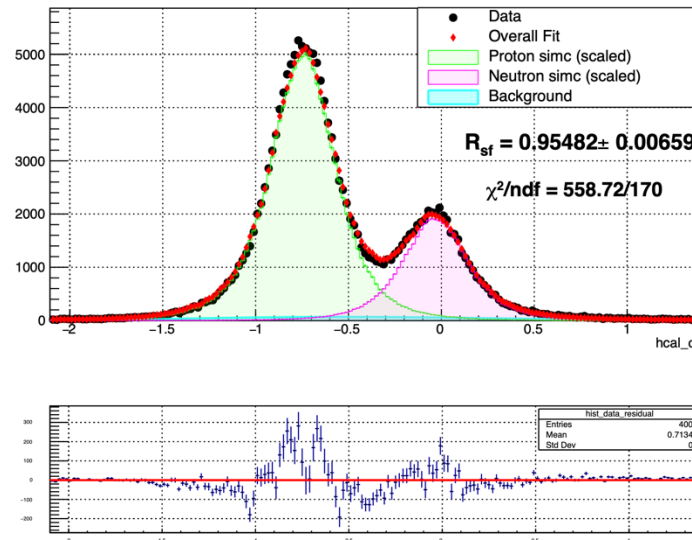
Inelastic Contamination: $Q^2 = 3 \text{ (GeV/c)}^2$

$Q^2 = 3 \text{ (GeV/c)}^2$

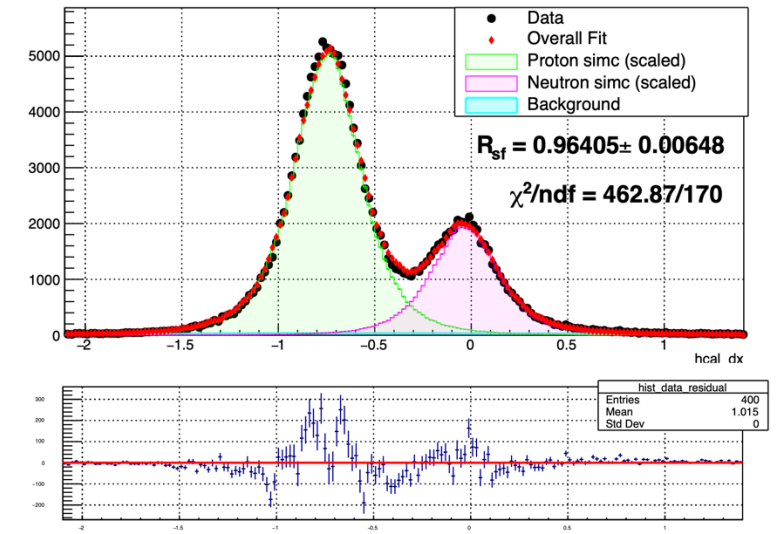
Plots Credit: **Maria Satnik**



2nd Order Polynomial



Bg. Shape from Data



Inelastic MC Generator

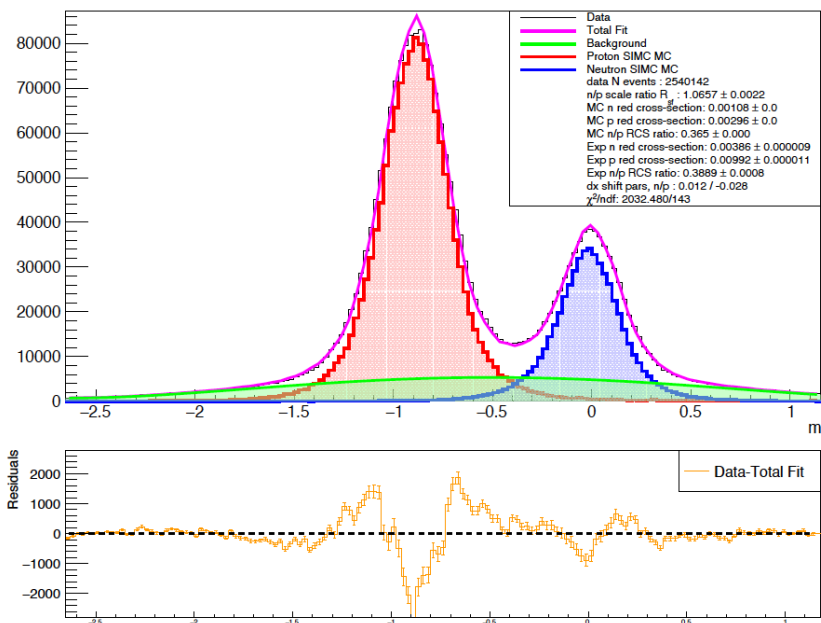
❖ $R_{n/p}^{sf}$ values obtained using different background models agree within **1%**.

Inelastic Contamination: $Q^2 = 4.5 \text{ (GeV/c)}^2$

$Q^2 = 4.5 \text{ (GeV/c)}^2$, high ϵ

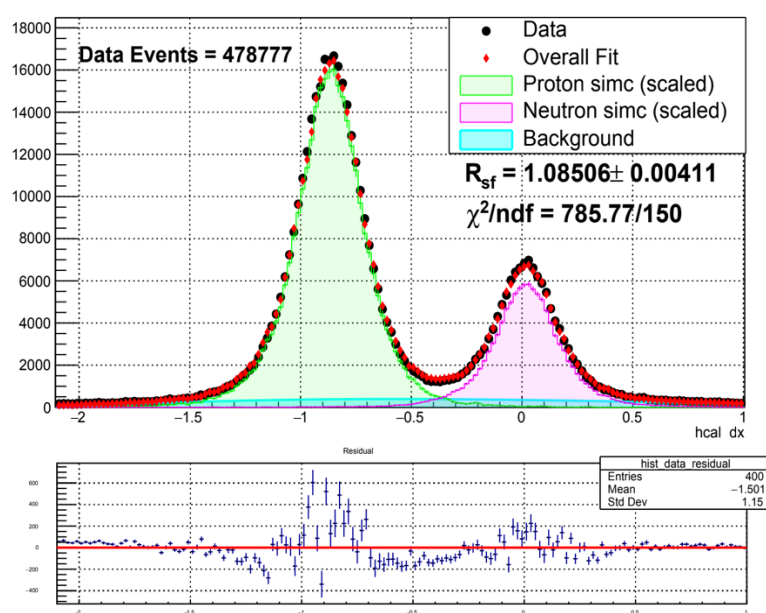
Plots Credit: **Zeke Wertz, Maria Satnik**

dx, shifitit poly4 BG



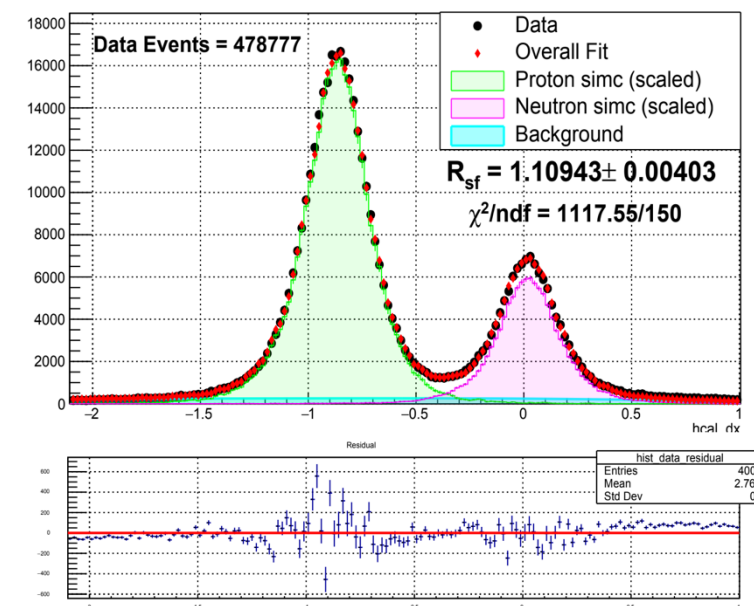
4th Order Polynomial

hcal dx



Bg. Shape from Data

hcal dx

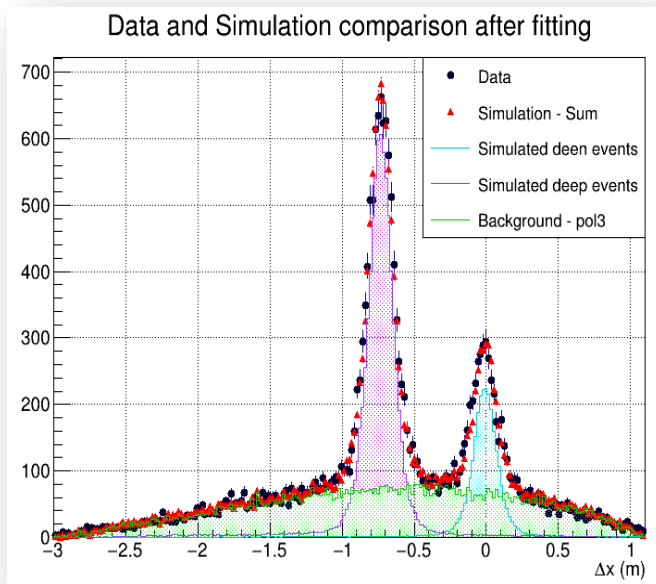


Inelastic MC Generator

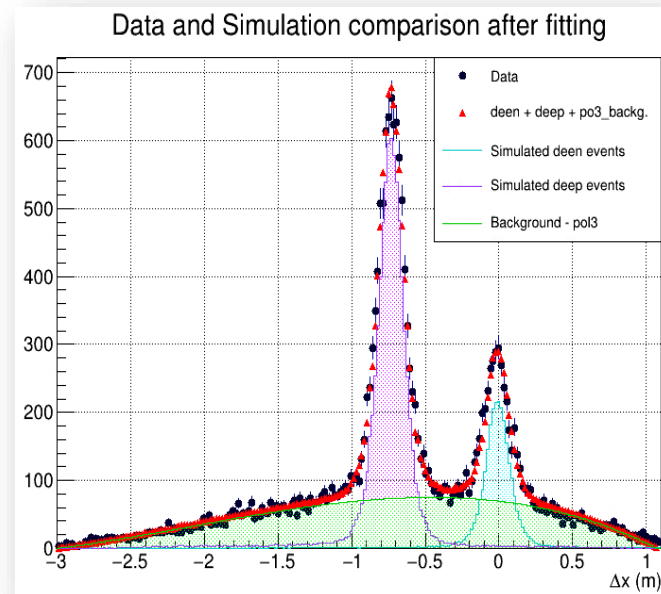
Inelastic Contamination: $Q^2 = 13.6 \text{ (GeV/c)}^2$

$Q^2 = 13.6 \text{ (GeV/c)}^2$

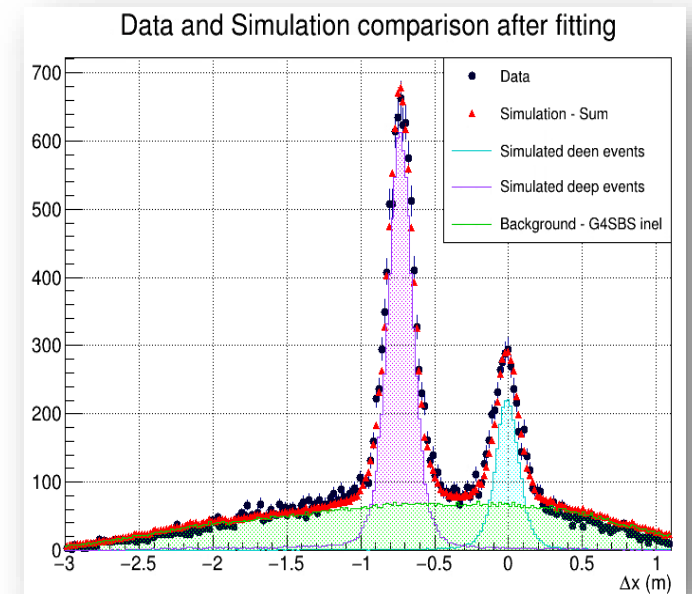
Plots Credit: **Anuruddha Rathnayake**



3rd order polynomial “fixed”



3rd order polynomial: all parms. allowed to vary



Inelastic MC

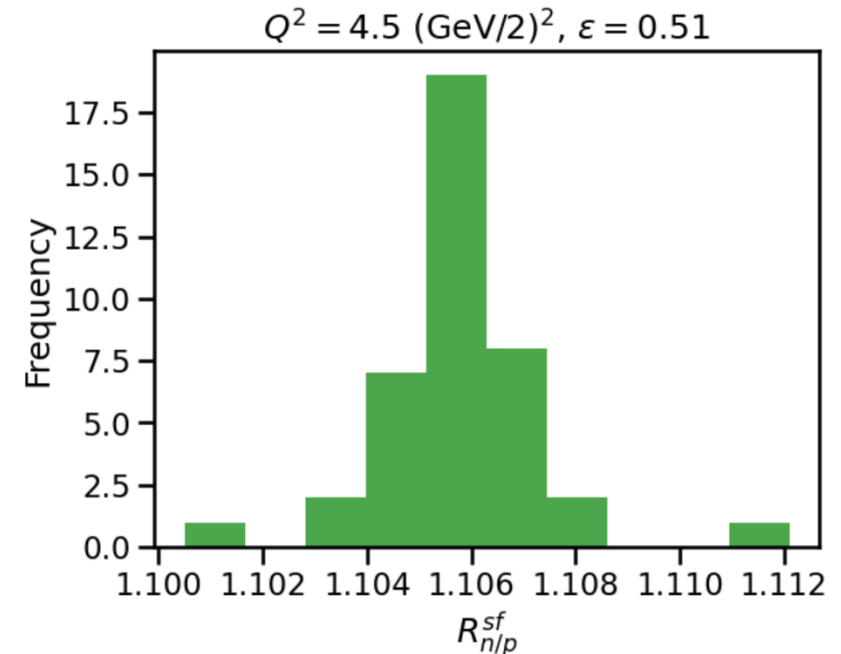
Sources of Systematic Uncertainty

- Inelastic Contamination
- **Cut Stability**
- HCAL Nucleon Detection Efficiency (NDE)

Cut Stability: $Q^2 = 4.5 \text{ (GeV/c)}^2$, low ϵ

- The choice of optimal cut region has some associated uncertainty.
- We vary each cut range by +10% and -10% while keeping the other cuts constant at their optimized values. Then, for each variation extract $R_{n/p}^{sf}$.
- One standard deviation of the resulting $R_{n/p}^{sf}$ distribution is quoted as the associated systematic uncertainty.

$Q^2 = 4.5 \text{ (GeV/c)}^2$, low ϵ



Sources of Systematic Uncertainty

- Inelastic Contamination
- Cut Stability
- HCAL Nucleon Detection Efficiency (NDE)

HCAL Proton Detection Efficiency (ϵ_{pDE}) from Data

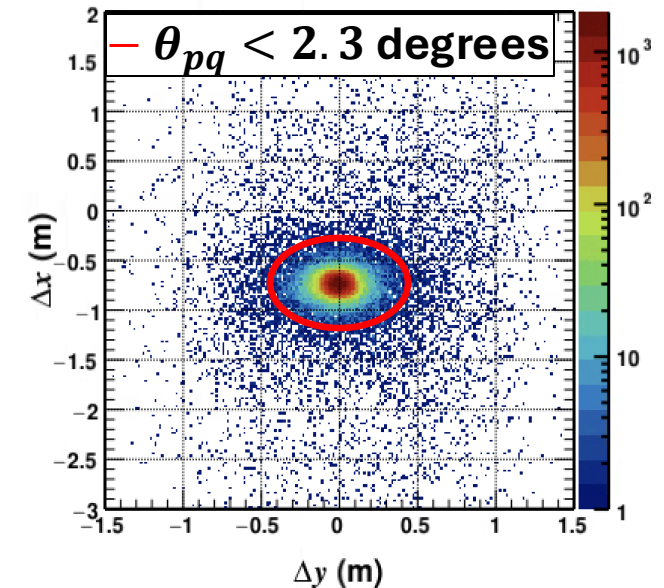
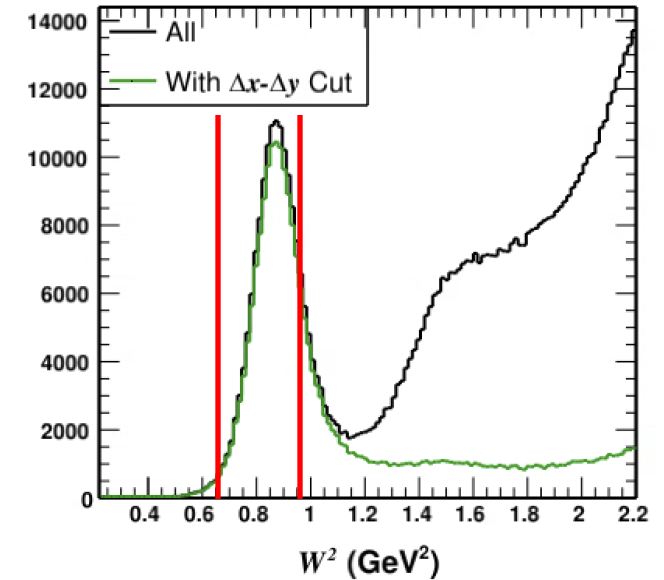
Methodology:

- Efficiency is defined as:

$$\epsilon_{HCAL}^p = \frac{\text{Number of proton events detected by HCAL}}{\text{Number of proton events expected to hit HCAL}}$$

- Use LH2 data from low- Q^2 kinematics, namely 3 and 4.5 (GeV/c)²
- Select elastic ep events with very strict W_2 cut to ensure that the background contamination is not statistically significant.
- Get the total number of proton events **expected to hit HCAL** to form the **denominator**. Apply all electron arm cuts including the fiducial cut. **No cuts involving HCAL are applied.**
- Get the total number of proton events **detected by HCAL** with additional cuts on HCAL energy and θ_{pq} to form the **numerator**.
- Calculate statistical error using binomial method:

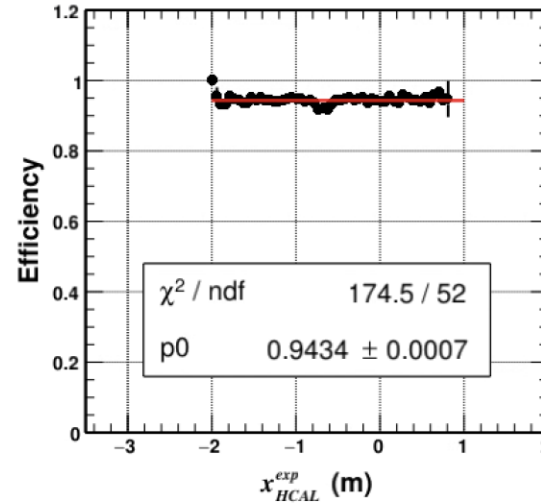
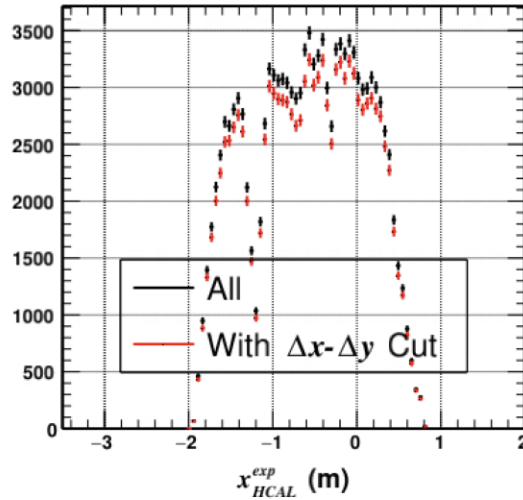
$$\sigma_{\epsilon_{HCAL}} = \left[\frac{\epsilon_{HCAL}(1 - \epsilon_{HCAL})}{\text{Denominator}} \right]^{\frac{1}{2}}$$



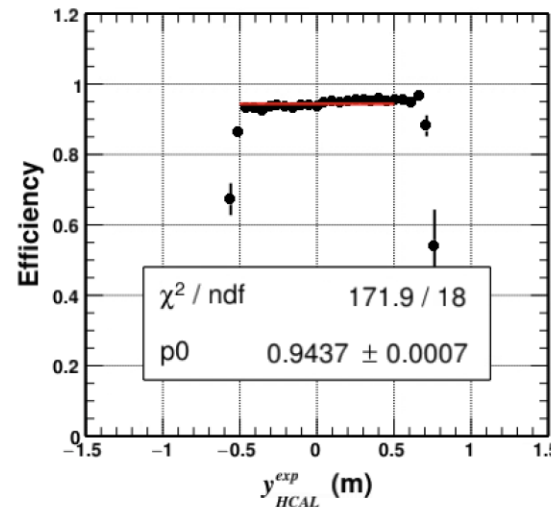
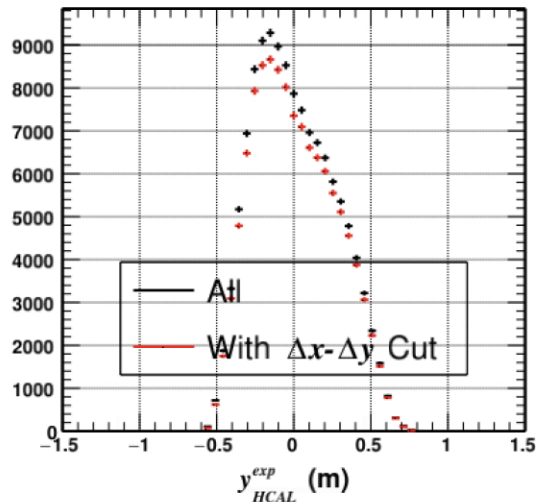
HCAL pDE form Data: Results

$Q^2 = 3 \text{ (GeV/c)}^2$

Dispersive



Non-Dispersive

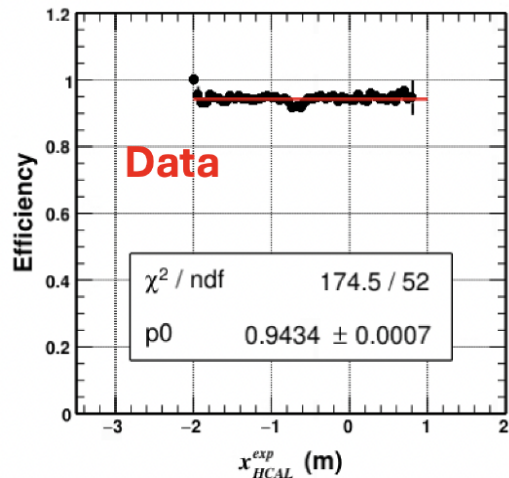


- The observed acceptance averaged efficiency value is very high in both dispersive and non-dispersive directions, as expected.
- No non-uniformity observed in the non-dispersive direction.
- A hint of non-uniformity in the dispersive direction around -0.6 m, near the middle of HCAL acceptance.

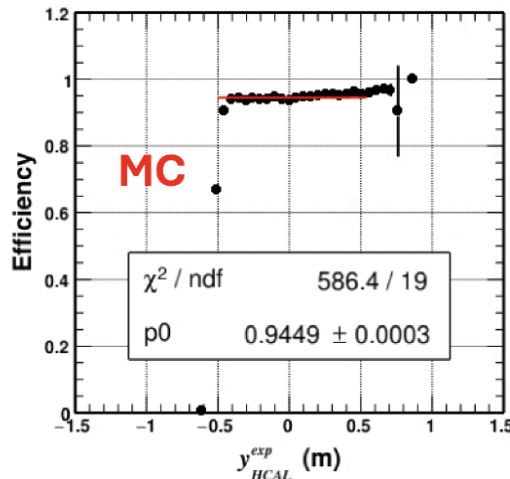
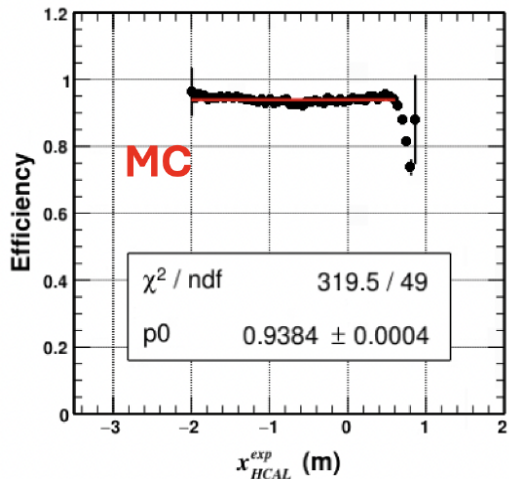
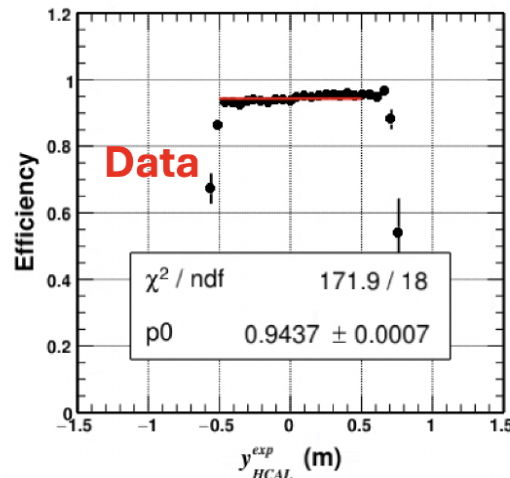
HCAL pDE: Data/MC Comparison

$$Q^2 = 3 \text{ (GeV/c)}^2$$

Dispersive



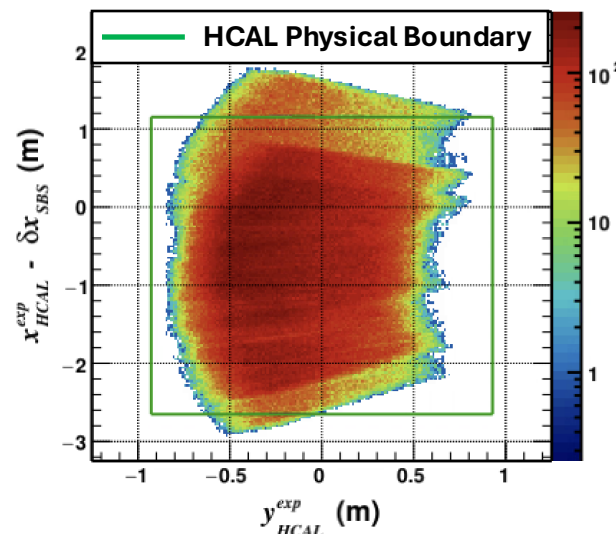
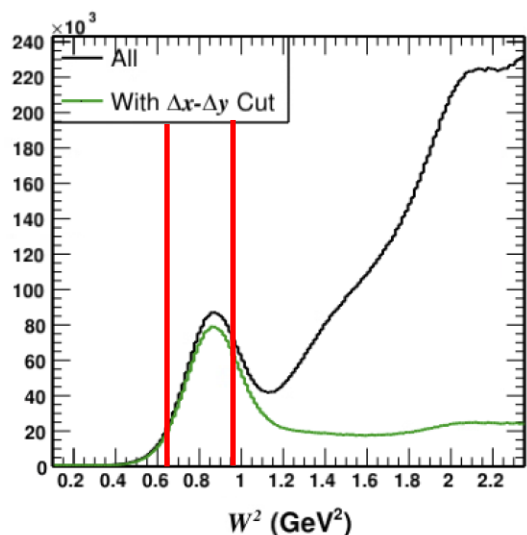
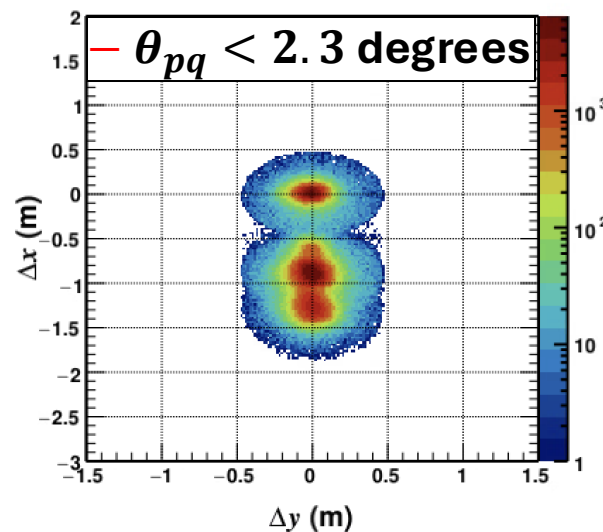
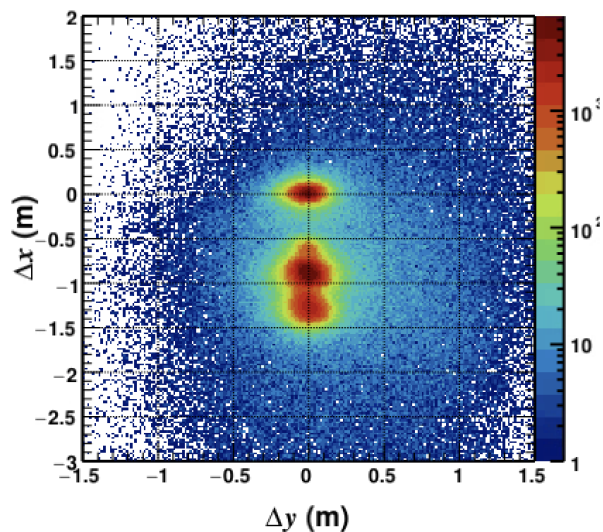
Non-Dispersive



- The observed acceptance averaged efficiency values closely align between data and MC, which is reassuring.
- The efficiency non-uniformity in the dispersive direction present in data is not observed in MC.
- Such non-uniformity affects $R_{n/p}^{sf}$ and therefore must be corrected.
- There are several ways to handle this. One approach is to modify the MC event weights based on the non-uniformity observed in data.

HCAL pDE: Tackling Non-Uniformity w/ Efficiency Map

$Q^2 = 4.5 \text{ (GeV/c)}^2$, high ϵ

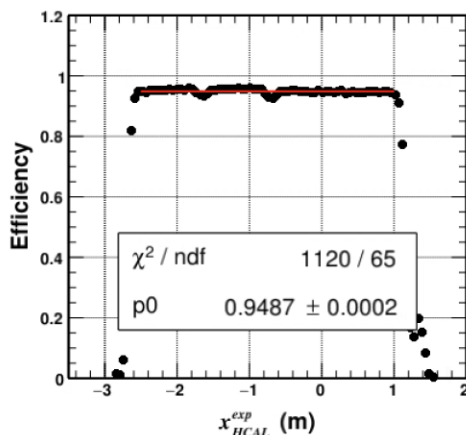
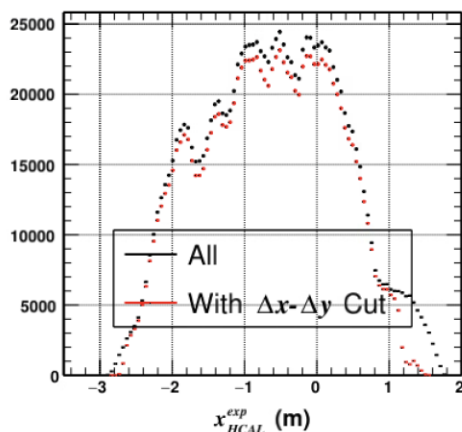


- **Goal:** Create an efficiency map based on real data that captures HCAL efficiency non-uniformity across the entire acceptance.
- LH2 data from one SBS field settings won't cover the entire acceptance of HCAL.
- Combined LH2 data from 4 different SBS field settings taken at 4.5 (GeV/c)^2 , high ϵ kinematics, in a self-consistent way.
- With this dataset, performed the same analysis discussed before to get HCAL pDE.

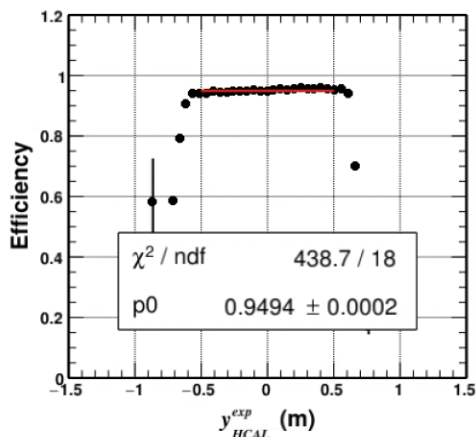
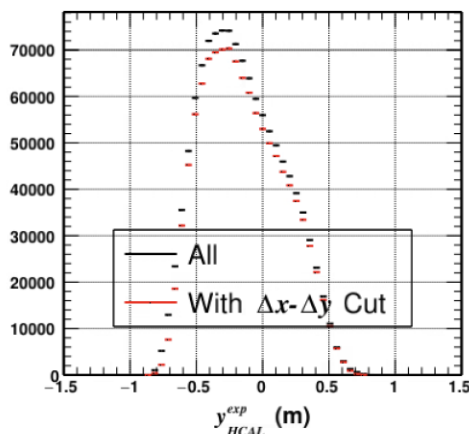
HCAL pDE: Tackling Non-Uniformity w/ Efficiency Map

$Q^2 = 4.5$ (GeV/c)² (high ϵ), SBS Field Strength: 0%, 50%, 70%, 100%

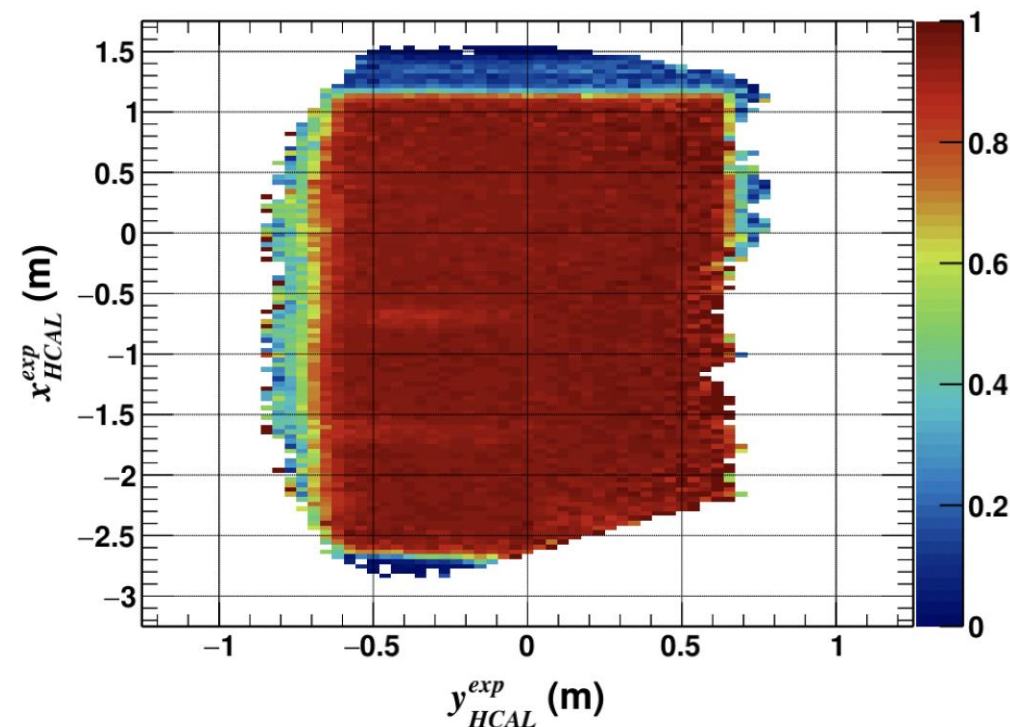
Dispersive



Non-Dispersive



Efficiency Map

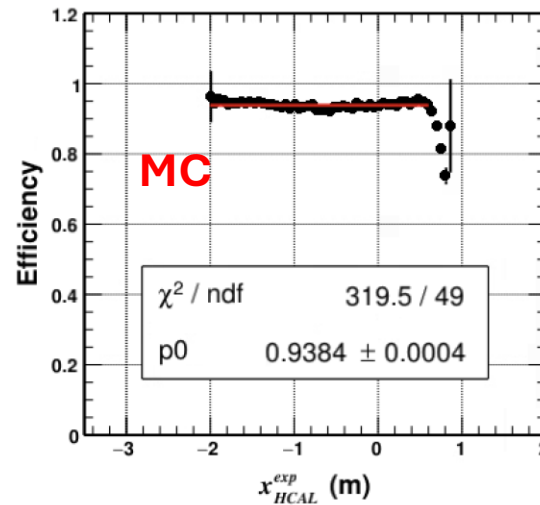
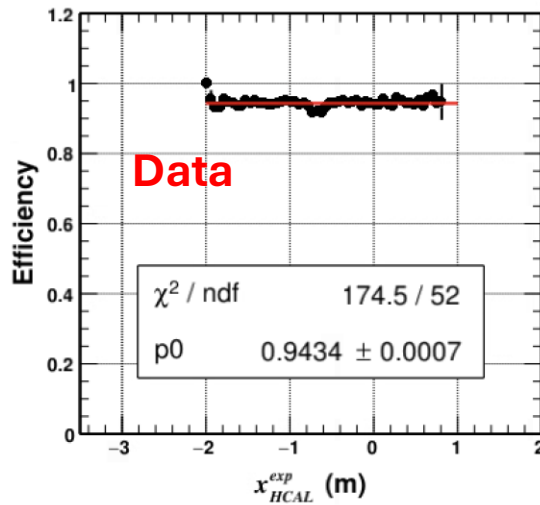


- Relative efficiency correction factor:

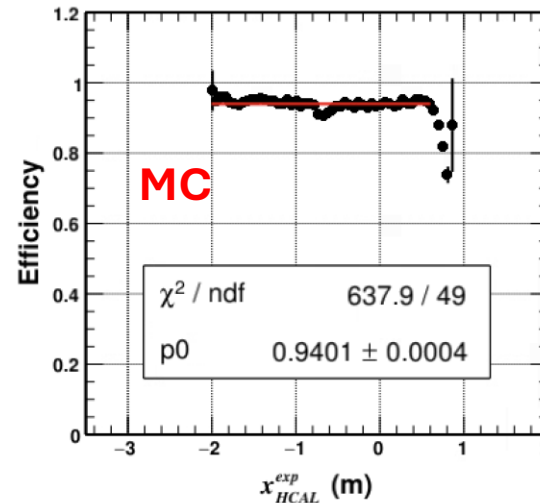
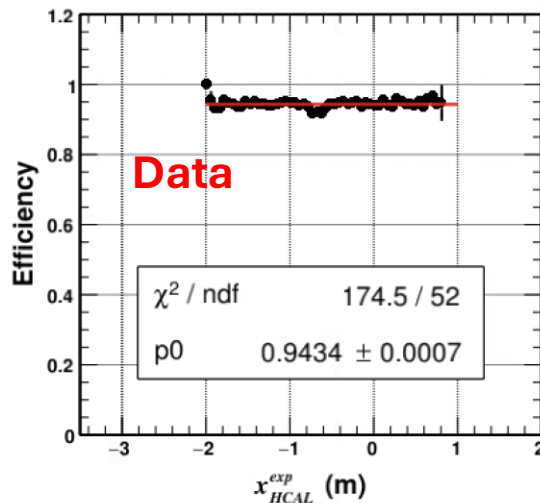
$$c = \frac{\epsilon_{HCAL}^p(y_{HCAL}^{exp}, x_{HCAL}^{exp})}{\langle \epsilon_{HCAL}^p \rangle}$$

HCAL pDE: Data/MC Comparison with Correction

Before Correction



After Correction



- Efficiency correction effectively accounts for the non-uniformities observed in the data, ensuring they are reproduced in MC.
- $R_{n/p}^{sf}$ is extracted both with and without the efficiency correction.
- The difference is quoted as the associated systematic uncertainty.
- ❖ **Caveats:**
 - We cannot extract proton detection efficiency reliably from data at higher Q^2 kinematics.
 - There is no obvious way to calibrate neutron detection efficiency from data.

Total Systematic Error Budget

From My Independent Analysis

Table III: Total systematic error budget for λ_{GMN} kinematics. The Q^2 and ϵ values are central values, with Q^2 quoted in $(\text{GeV}/c)^2$. Among the systematic error sources, inel. represents inelastic contamination, NDE refers to the HCAL nucleon detection efficiency, and cut s. indicates cut stability. Errors associated with individual sources have been added in quadrature to calculate the total error.

	Error Sources	Q^2 (ϵ)				
		3 (0.72)	4.5 (0.51)	7.4 (0.46)	9.9 (0.50)	13.6 (0.41)
$\Delta(R)_{\text{sys}}$	Inel.	0.0014	0.0056	0.0030	0.0045	0.0130
	NDE	0.0004	0.0007	0.0011	0.0011	0.0040
	Cut S.	0.0006	0.0006	0.0015	0.0024	0.0020
	Total	0.0016	0.0057	0.0036	0.0052	0.0137
$\Delta\left(\frac{G_M^n}{\mu_n G_D}\right)_{\text{sys}}$	Inel.	0.0019	0.0068	0.0035	0.0049	0.0139
	NDE	0.0005	0.0009	0.0012	0.0012	0.0043
	Cut S.	0.0008	0.0007	0.0018	0.0027	0.0022
	σ_{Red}^p	0.0080	0.0090	0.0123	0.0129	0.0102
	G_E^n	0.0053	0.0061	0.0054	0.0052	0.0038
	Total	0.0098	0.0129	0.0140	0.0150	0.0183

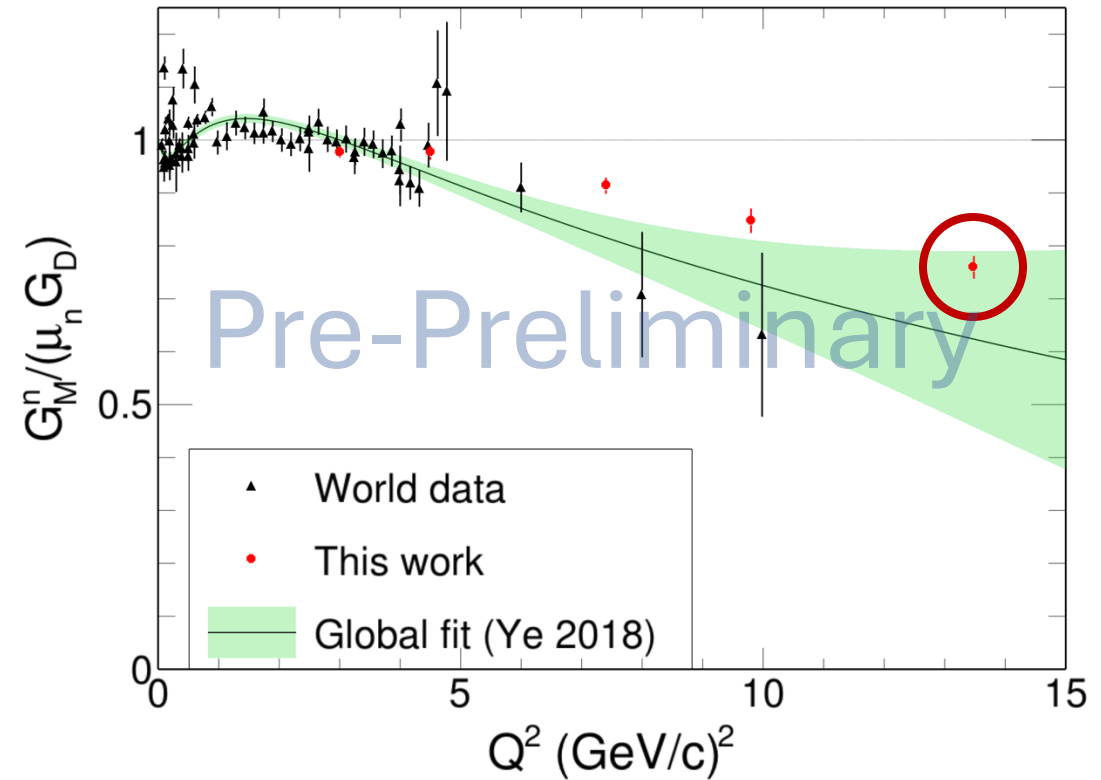
- Brief Overview
- Physics Analysis Methodology
- Extraction of Experimental Observable
- Systematic Uncertainty Quantification
- **Preliminary Results**
- Summary and outlook

Preliminary Results

From My Independent Analysis

Table IV: Final results. $\langle Q^2 \rangle$ and $\langle \epsilon \rangle$ are the acceptance averaged Q^2 and ϵ , respectively.

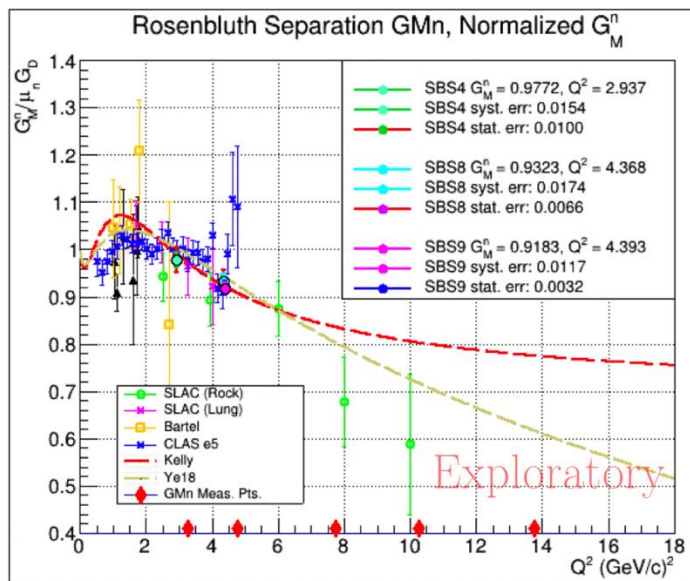
$\langle Q^2 \rangle$	$\langle \epsilon \rangle$	$R \pm \Delta(R)_{stat} \pm \Delta(R)_{sys}$	$\frac{G_M^n}{\mu_n G_D} \pm \Delta(\frac{G_M^n}{\mu_n G_D})_{stat} \pm \Delta(\frac{G_M^n}{\mu_n G_D})_{sys}$
2.989	0.722	$0.3808 \pm 0.0025 \pm 0.0016$	$0.9774 \pm 0.0033 \pm 0.0098$
4.488	0.515	$0.4037 \pm 0.0011 \pm 0.0057$	$0.9763 \pm 0.0014 \pm 0.0129$
7.464	0.469	$0.3974 \pm 0.0035 \pm 0.0036$	$0.9071 \pm 0.0042 \pm 0.0140$
9.834	0.502	$0.3868 \pm 0.0154 \pm 0.0052$	$0.8473 \pm 0.0173 \pm 0.0150$
13.465	0.417	$0.3615 \pm 0.0100 \pm 0.0137$	$0.7582 \pm 0.0107 \pm 0.0183$



- Statistical and Systematic errors have been added in quadrature.
- The most significant sources of systematics have been considered, though this list is not exhaustive. Other factors, such as final state interactions, will also contribute to the uncertainties. Efforts are ongoing to quantify these effects.

Preliminary Results contd.

Credit: John B., April 2024



Credit: Sebastian S., July 2024

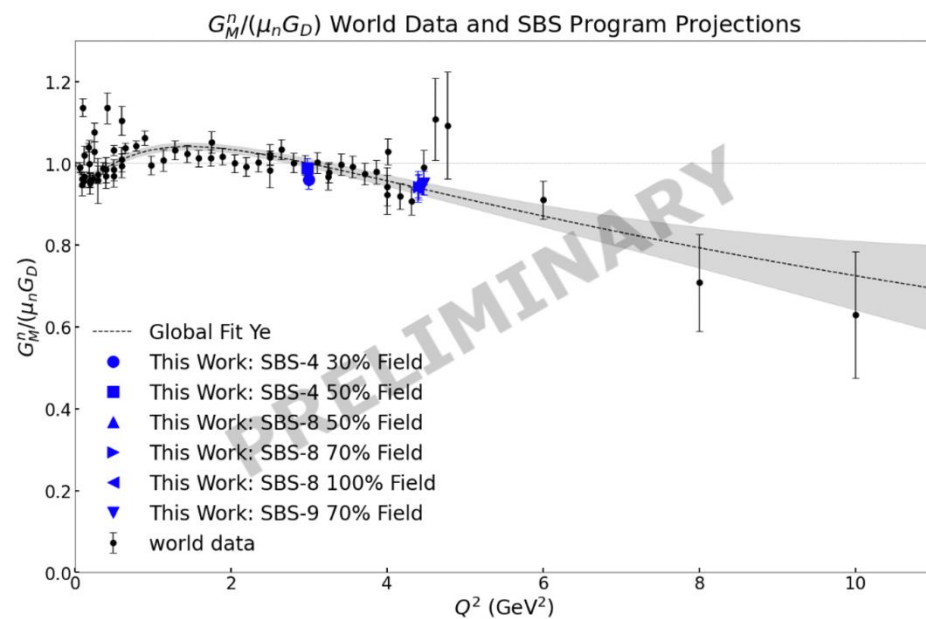
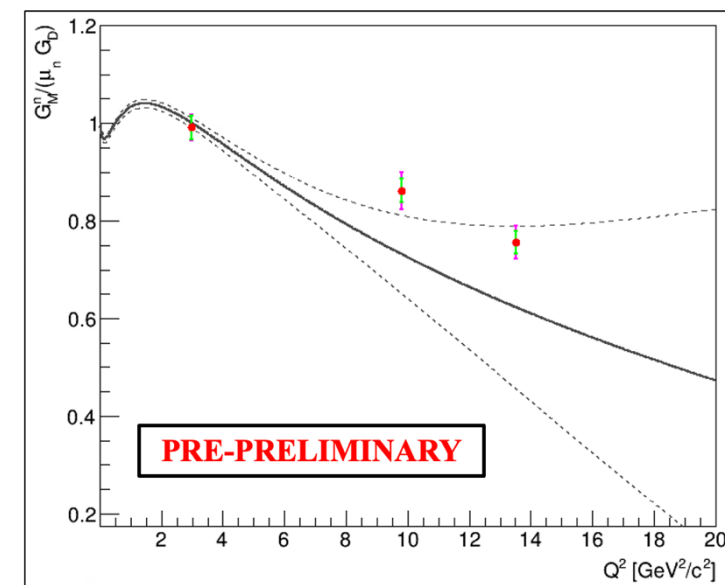


Figure 109: $G_M^n / (\mu_n G_D)$ extractions from this work plotted along with world data taken from [87] and Ye et al. fit [184].

Credit: Anu R., Sep 2024



- **Grey curve:** global data parameterization for GMn, Ye – 2018
- **Green error bounds:** systematic error
- **Magenta error bounds extending from green:** statistical error

- Preliminary results obtained from independent analyses are consistent with each other.

Summary, Outlook, & Acknowledgements

- A significant analysis effort, carried out by a large and active analysis group, is ongoing and edging close to publication.
- Sophisticated analysis machinery including realistic MC event generators are in place.
- Independent analysis efforts are showing consistent results.
- A few shortcomings associated to detector calibration has been noticed and efforts are ongoing to improve those. The third and the last pass of calibration fine tuning should begin shortly.
- The extraction of the final results will proceed promptly, as the analysis framework is already in place, paving the way for publication. *My guess would be within a year!*
- ❖ I would like to thank the entire Hall A collaboration and of course the SBS collaboration and anyone else who has contributed to the success of SBS-GMn.
- ❖ I would also like to thank the US Department of Energy Office of Science, Office of Nuclear Physics, for supporting this work (Award ID DE-SC0021200).



Thank You for Your Attention!
Questions? Comments?

DNP 2023 - Team SBS in Hawaii!!